

# A Crash Course in Quantum Transport II: Various Mesoscopic Interactions

**Kongju National University  
Dept. of Physics Education**

**Sang-Jun Choi**

**Summer School of Mesoscopic Physics  
@PKNU, 2025. 5. 24**



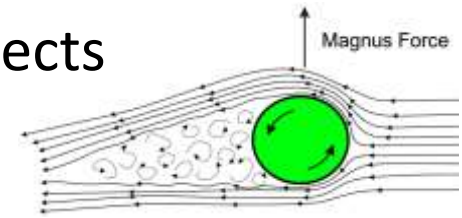
# What is Mesoscopic Quantum Transport

- Mesoscopic quantum **transport**?

- Why **'transport?'**

→ Transport reveals information of transported objects

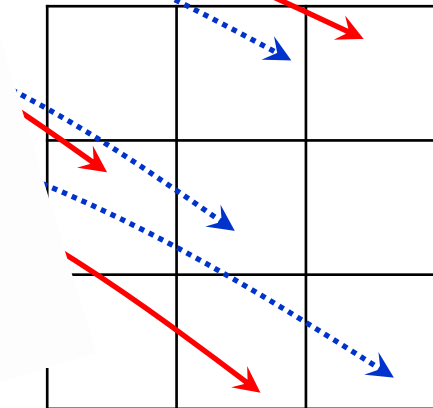
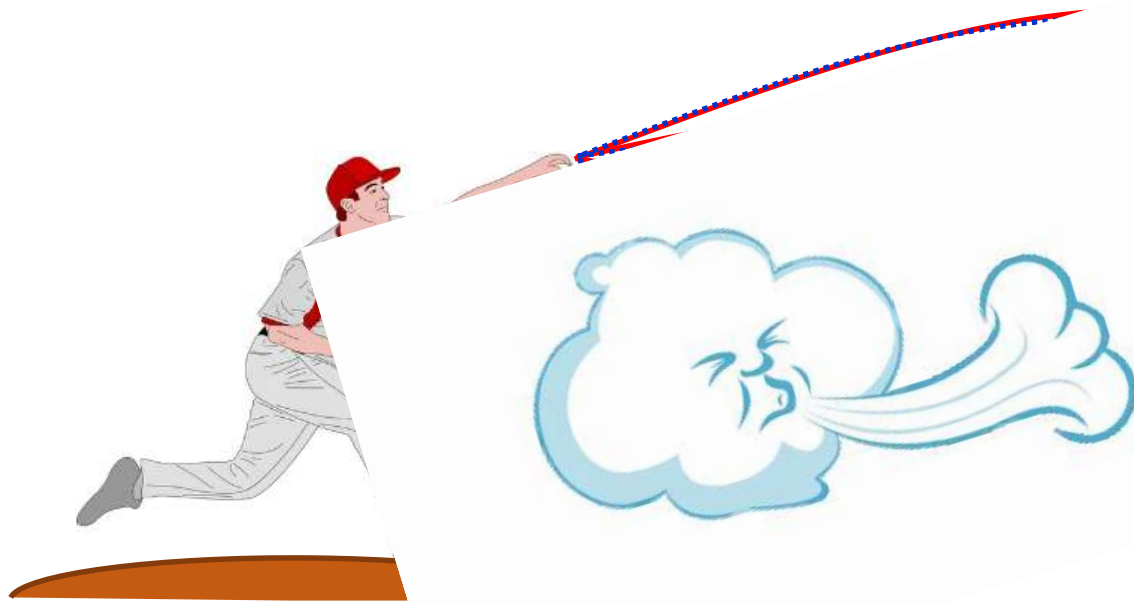
→ Imagine we are in a dark room!



**Interaction b/t ball & wind**

**Spin**

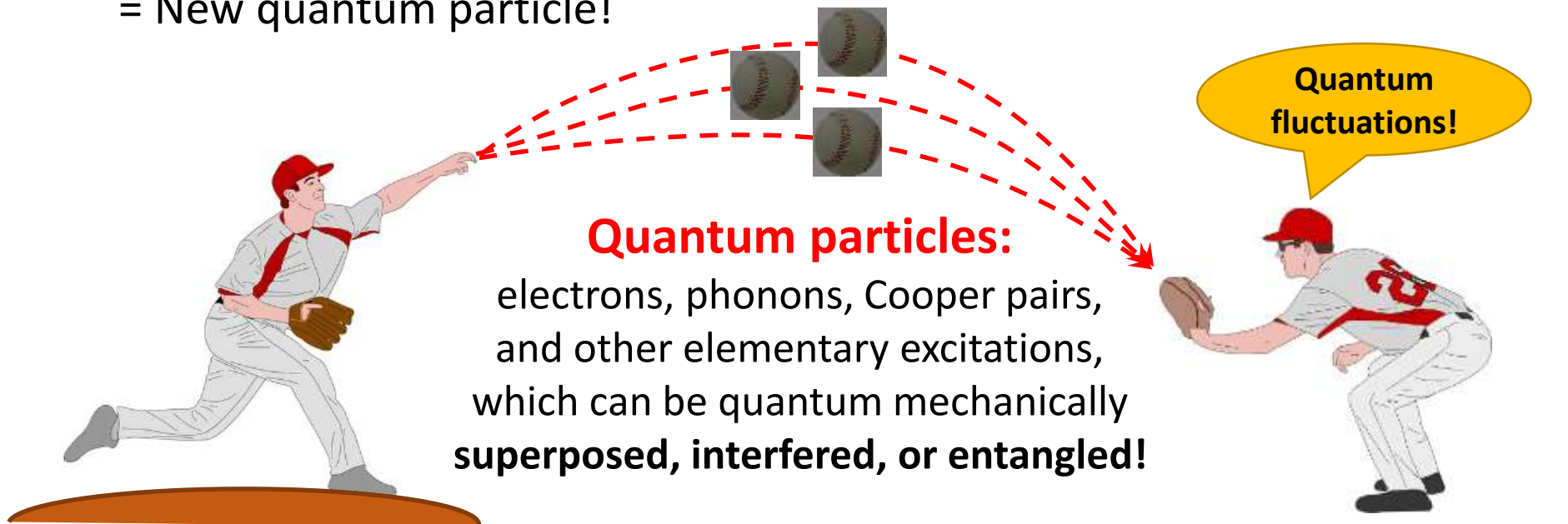
of the ball



Figures from depositphotos.com

# What is Mesoscopic Quantum Transport

- Mesoscopic **quantum transport**?
- Why **'transport'**: Transport reveals information of transported objects
- Which one is **'quantum'**: ptls are superposed, interfered, or entangled  
→ New phenomena with the same game setting?  
= New quantum particle!



Figures from depositphotos.com

# What is Mesoscopic Quantum Transport

- **Mesoscopic quantum transport?**
- **Why ‘transport’**: Transport reveals information of transported objects
- **Which one is ‘quantum’**: ptls are superposed, interfered, or entangled
- **What’s meso-scopic systems**
  - **Playground** for quantum baseballs (not too large: macro-scopic) but **well-controllable & designable** (not too small: micro-scopic)

We can place **quantum** pitchers, catchers, fans on the field, as we want!



Competition  
b/t **various**  
scales matter!

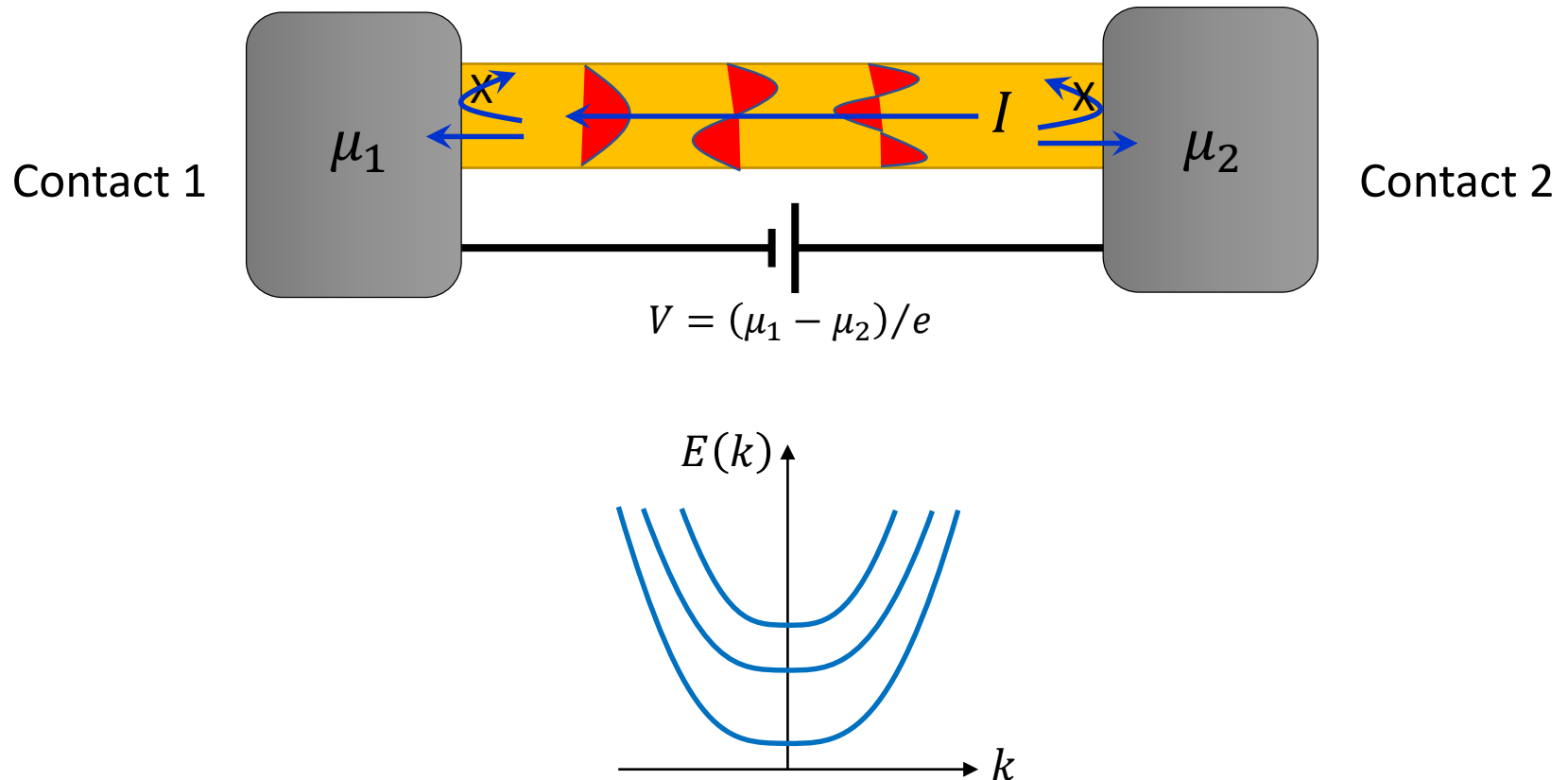


# Physics of MQT: perfect conductor

- **Perfect conductor**

**we assume:** size of conductor,  $L \ll L_m, L_\phi$ . But  $\lambda_F < W$  w/ subbands

Reflectionless contacts (no backscattering at contact)



# Physics of MQT: perfect conductor

- Perfect conductor

**we assume:** size of conductor,  $L \ll L_m, L_\phi$ . But  $\lambda_F < W$  w/ subbands

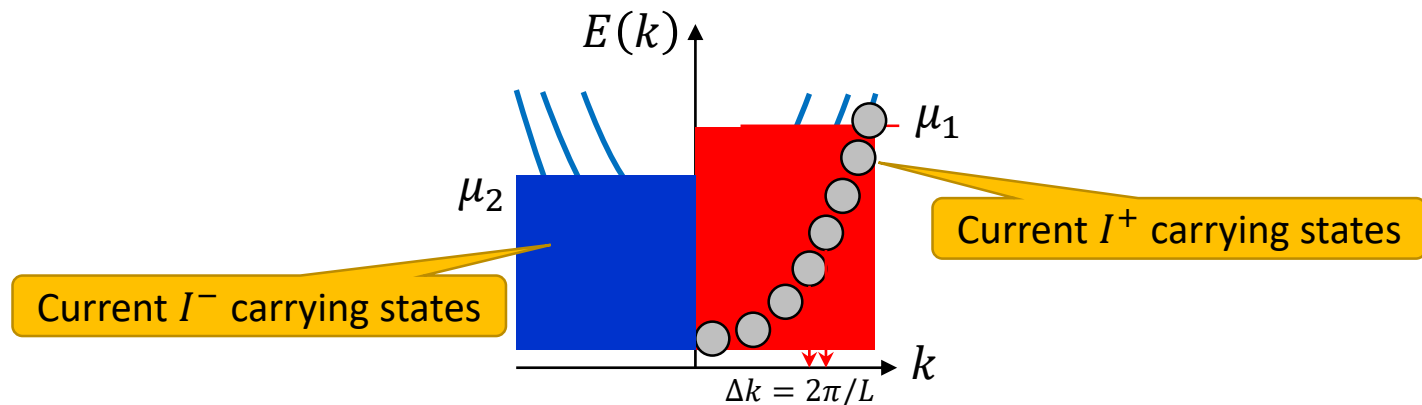
Reflectionless contacts (no backscattering at contact)

- Calculating the current

(zero temp.)

$$I^+ = \frac{2e}{h} M \mu_1 \quad \& \quad I^- = -\frac{2e}{h} M \mu_2$$

Opposite sign due to opposite group velocity



# Physics of MQT: perfect conductor

- Perfect conductor

**we assume:** size of conductor,  $L \ll L_m, L_\phi$ . But  $\lambda_F < W$  w/ subbands

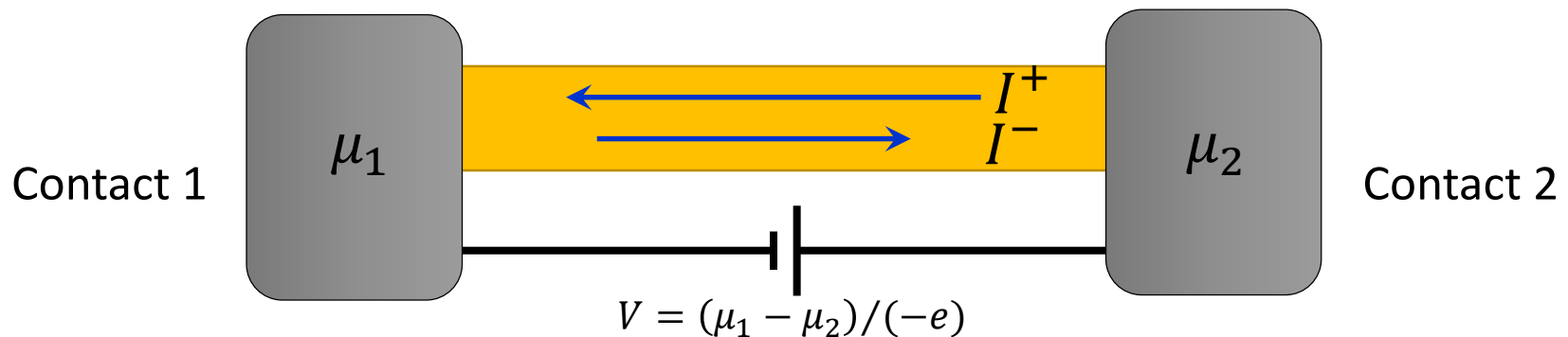
Reflectionless contacts (no backscattering at contact)

- Calculating the current

(zero temp.)  $I^+ = \frac{2e}{h} M \mu_1$  &  $I^- = -\frac{2e}{h} M \mu_2$

$$I = I^+ + I^- = \frac{2e}{h} M (\mu_1 - \mu_2) = \frac{2e^2}{h} M \frac{\mu_1 - \mu_2}{e} = \frac{2e^2}{h} M V$$

$G$  of a perfect conductor  
= integer multiple of  
conductance quantum



# Physics of MQT: perfect conductor

- Perfect conductor

**we assume:** size of conductor,  $L \ll L_m, L_\phi$ . But  $\lambda_F < W$  w/ subbands  
Reflectionless contacts (no backscattering at contact)

- Quantized conductance

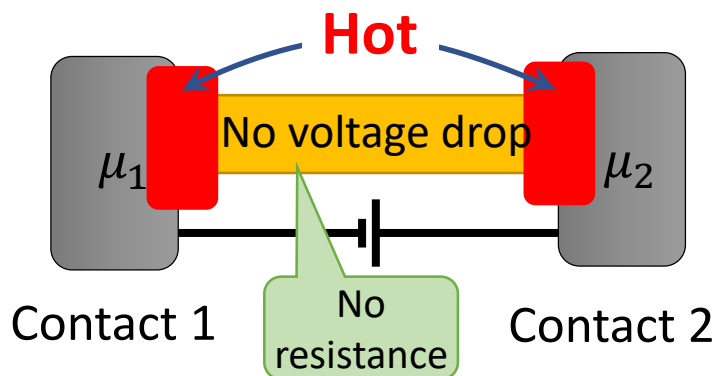
$$G = \frac{2e^2}{h} M$$

Contact resistance

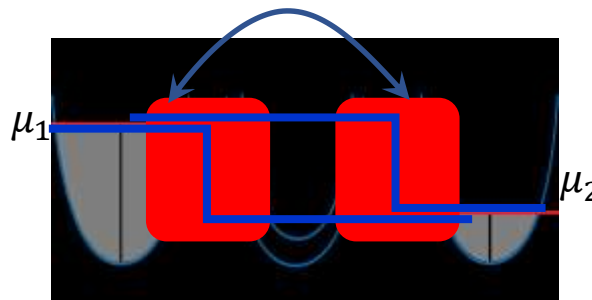
$$R_c = \frac{h}{2e^2 M} = \frac{12.9}{M} \text{ k}\Omega$$

- Where is the voltage drop?

**Ans.** at the contacts



Energy dissipation  
should occur to fit  
into B.C. at infinity



- i) Translational symmetry is broken at contacts
- ii) Contacts are irremovable

No matter how we define the voltage drop, it occurs **at the contacts**



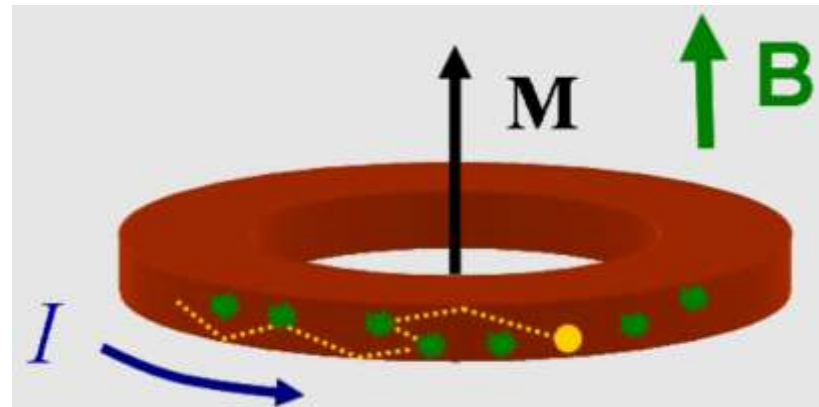
# Physics of MQT: perfect conductor

- **Perfect conductor**

**we assume:** size of conductor,  $L \ll L_m, L_\phi$ . But  $\lambda_F < W$  w/ subbands

Reflectionless contacts (no backscattering at contact)

- **Persistent Current & Scales**



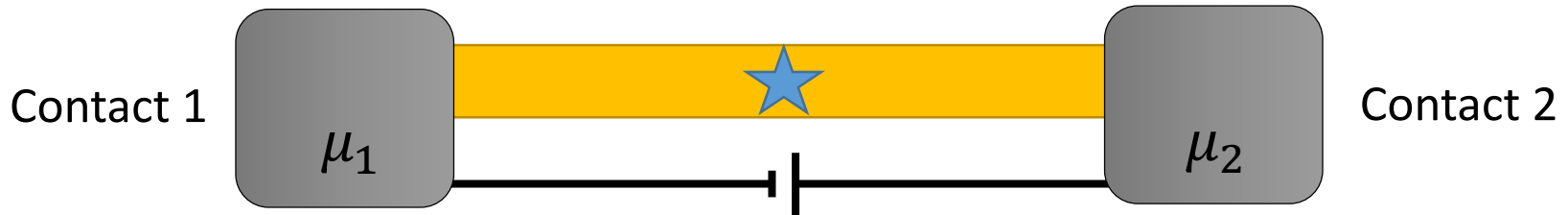
How long the time  
should be to be  
'persistent?'

M. Büttiker, Y. Imry, R. Landauer, *Josephson behavior in small normal one-dimensional rings*,  
Phys. Lett. A. **96**, 365 (1983)

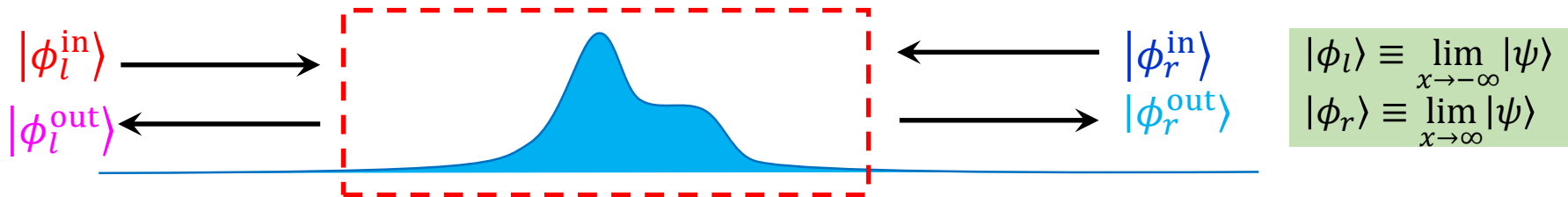
Measuring elusive "persistent current" that flows forever, R&D Daily. October 12, (2009)

# Physics of MQT: Not perfect but ballistic conductor

- **Ballistic conductor w/ a single impurity:** size of conductor,  $L \sim L_m$



- **Scattering Matrix**



General solution  $\hat{H}|\psi\rangle = E|\psi\rangle$ :  $|\phi_l\rangle = A|\phi_l^i\rangle + B|\phi_l^o\rangle$  &  $|\phi_r\rangle = C|\phi_r^o\rangle + D|\phi_r^i\rangle$ .

Undergraduate courses, we deal with two cases: (i) left & (ii) right incidence. We know

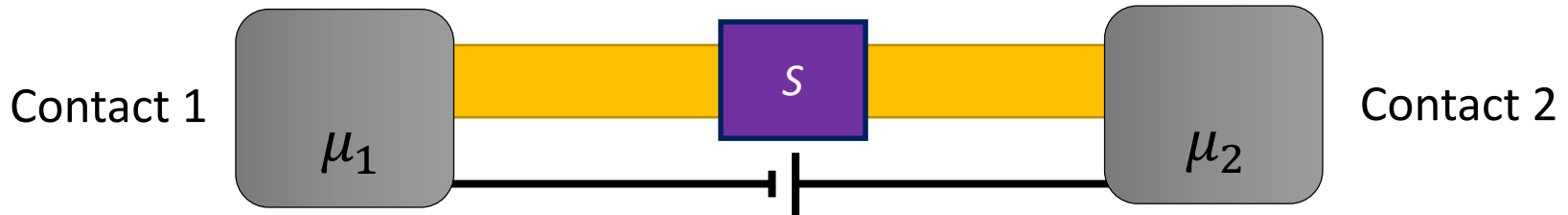
$$\begin{aligned} \text{(i) } B = rA \text{ \& } C = tA \text{ \& } D = 0: & \quad |\phi_l\rangle = A|\phi_l^i\rangle + rA|\phi_l^o\rangle \text{ \& } |\phi_r\rangle = tA|\phi_l^o\rangle \\ \text{(ii) } B = t'D \text{ \& } C = r'D \text{ \& } A = 0: & \quad + \left. \begin{aligned} |\phi_l\rangle = & \quad t'D|\phi_l^o\rangle \text{ \& } |\phi_r\rangle = r'D|\phi_r^o\rangle + D|\phi_r^i\rangle. \end{aligned} \right\} \end{aligned}$$

General solution is

$$|\phi_l\rangle = A|\phi_l^i\rangle + (rA + t'D)|\phi_l^o\rangle \text{ \& } |\phi_r\rangle = (tA + r'D)|\phi_r^o\rangle + D|\phi_r^i\rangle.$$

# Physics of MQT: Not perfect but ballistic conductor

- **Ballistic conductor w/ a single impurity:** size of conductor,  $L \sim L_m$



- **Scattering Matrix**



General solution:  $|\phi_l\rangle = A|\phi_l^i\rangle + (rA + t'D)|\phi_l^o\rangle$  &  $|\phi_r\rangle = (tA + r'D)|\phi_r^o\rangle + D|\phi_r^i\rangle$ .

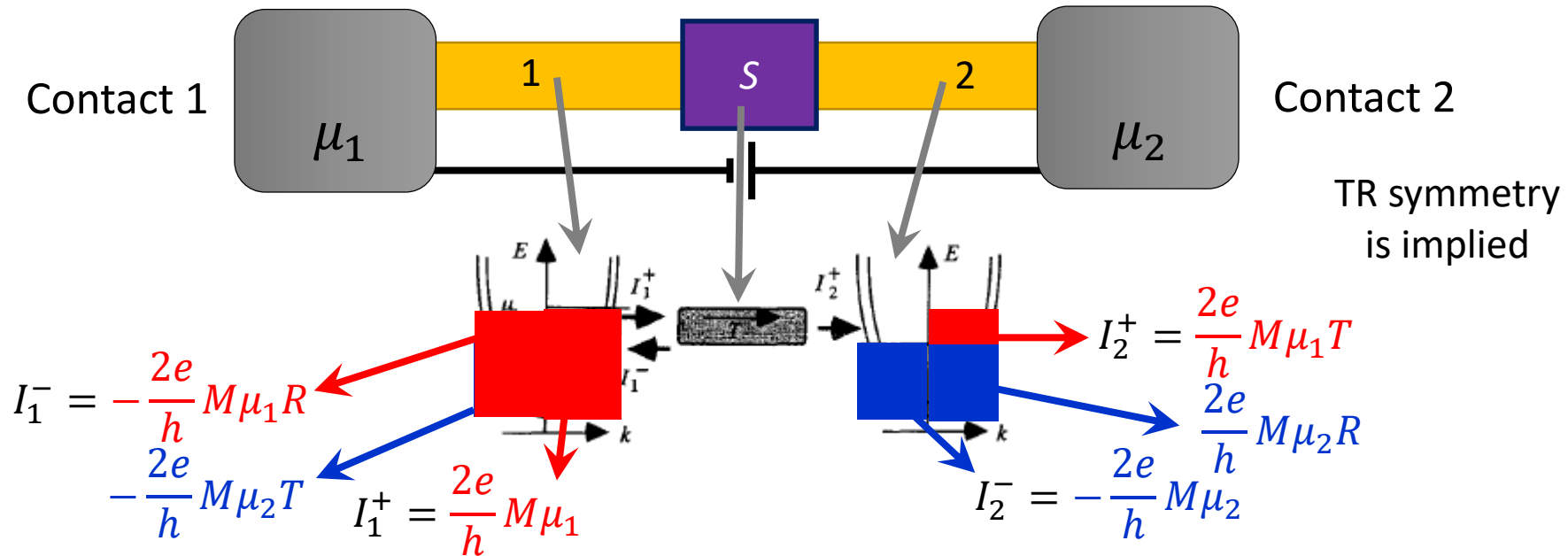
$$\begin{pmatrix} B \\ C \end{pmatrix} = \begin{pmatrix} r & t' \\ t & r' \end{pmatrix} \begin{pmatrix} A \\ D \end{pmatrix} = S \begin{pmatrix} A \\ D \end{pmatrix}$$

If interested only in amplitudes of scattering states at infinity, only thing we need to know is

$$S = \begin{pmatrix} r & t' \\ t & r' \end{pmatrix}$$

# Physics of MQT: Not perfect but ballistic conductor

- **Ballistic conductor w/ a single impurity:** size of conductor,  $L \sim L_m$



**Total current at lead 1:**

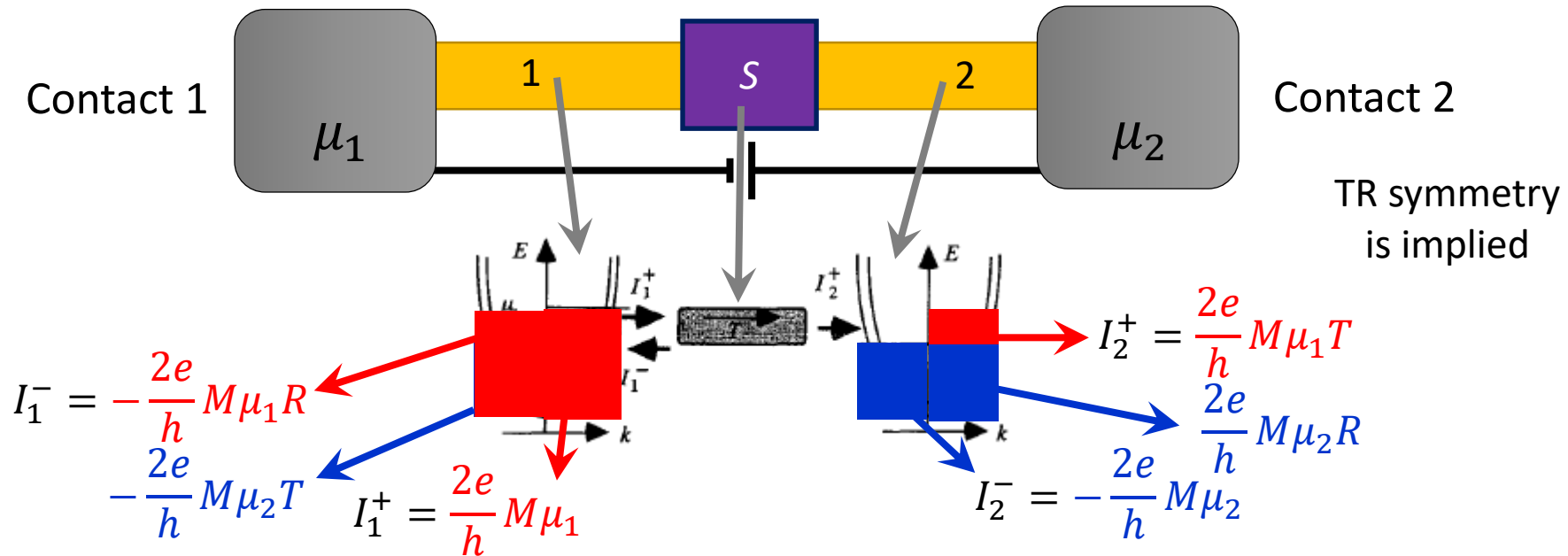
$$I_1 = I_1^+ + I_1^- = \frac{2e}{h} M \mu_1 - \frac{2e}{h} M \mu_1 (1 - T) - \frac{2e}{h} M \mu_2 T = \frac{2e}{h} M (\mu_1 - \mu_2) T$$

**Total current at lead 2:**

$$I_2 = I_2^+ + I_2^- = \frac{2e}{h} M \mu_1 T + \frac{2e}{h} M \mu_2 (1 - T) - \frac{2e}{h} M \mu_2 = \frac{2e}{h} M (\mu_1 - \mu_2) T$$

# Physics of MQT: Not perfect but ballistic conductor

- **Ballistic conductor w/ a single impurity:** size of conductor,  $L \sim L_m$



**Total current at lead 1&2:**

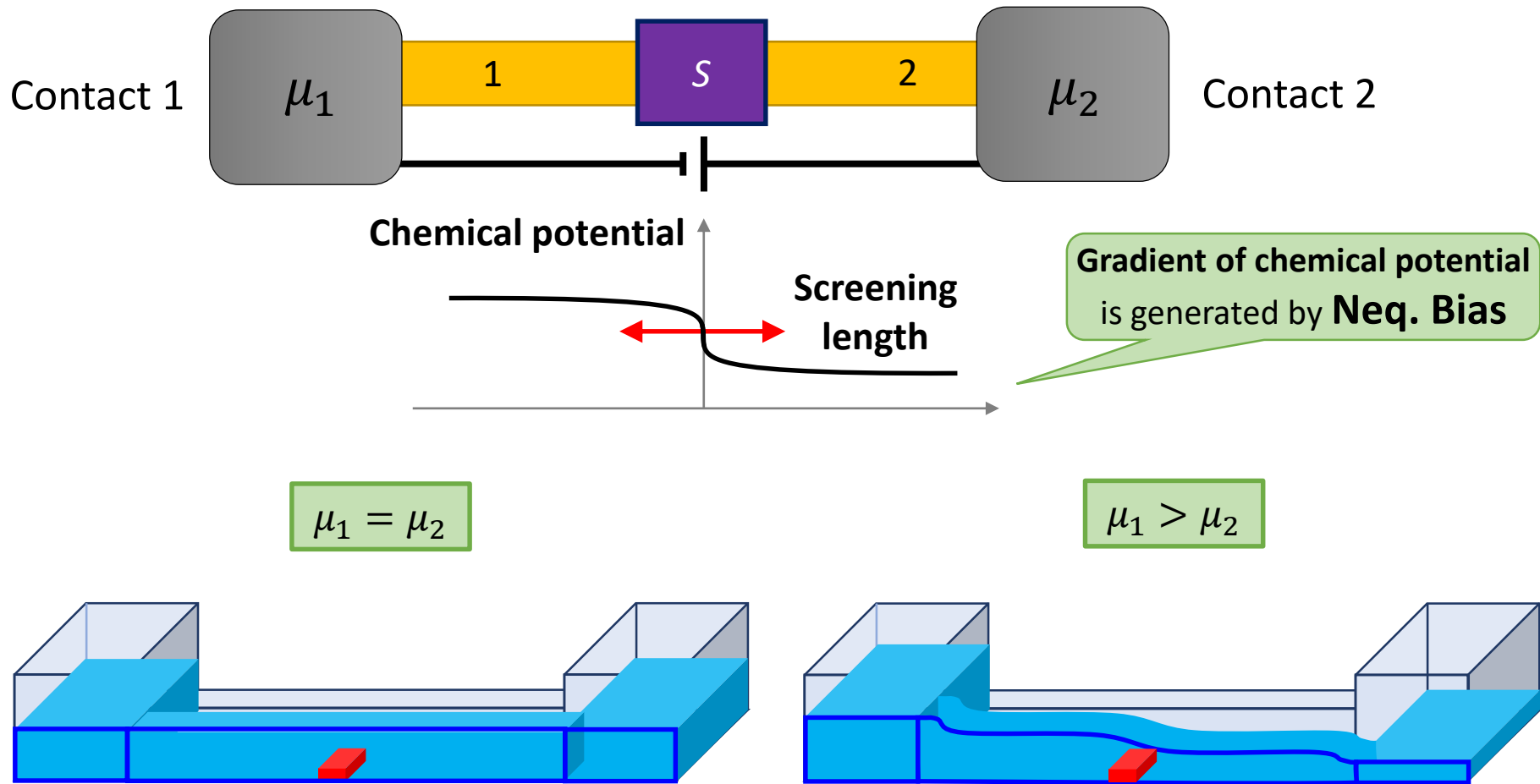
$$I = I_1 = I_2 = \frac{2e}{h} M (\mu_1 - \mu_2) T = \frac{2e^2}{h} M T \left( \frac{\mu_1 - \mu_2}{e} \right) = \frac{2e^2}{h} M T V$$

$$G = \frac{2e^2}{h} M T$$

Perfect  
conductor  
 $T = 1$

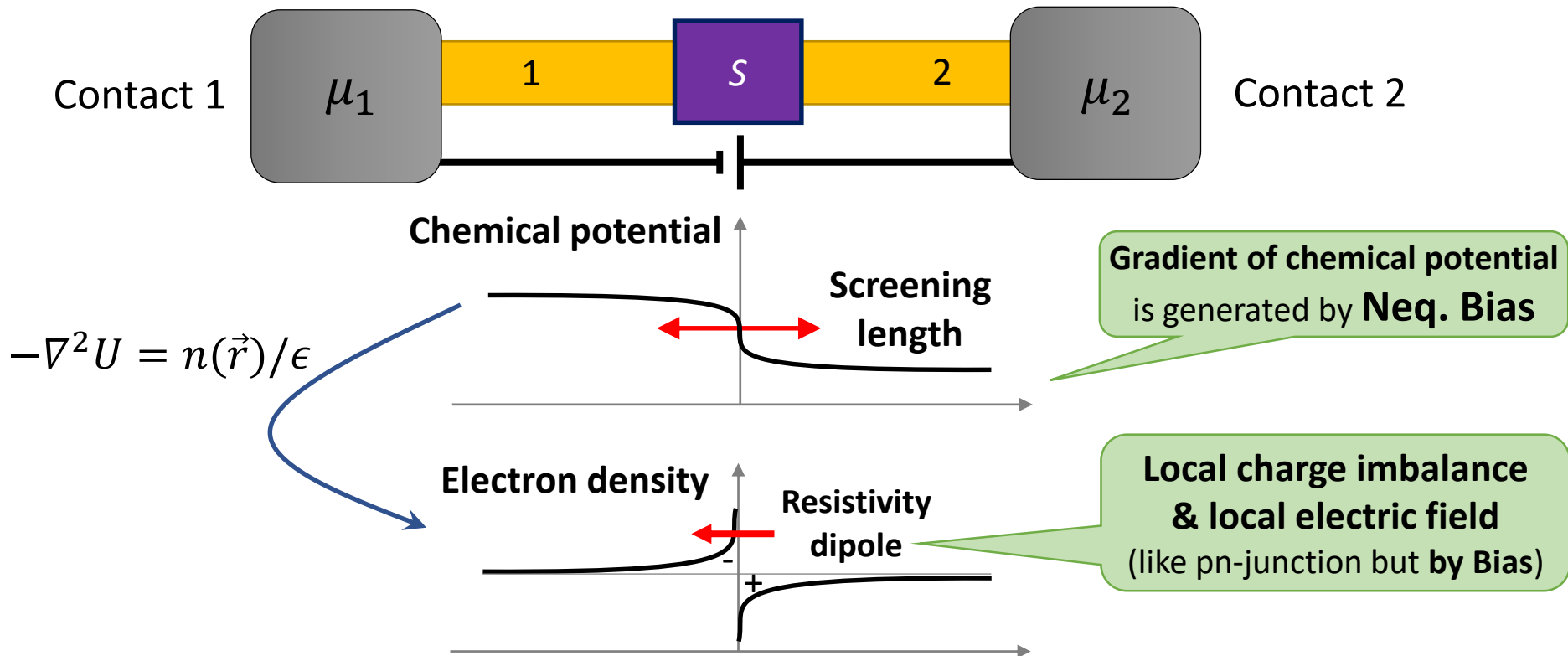
# Physics of MQT: Not perfect but ballistic conductor

- What is the electric field in the conductor?



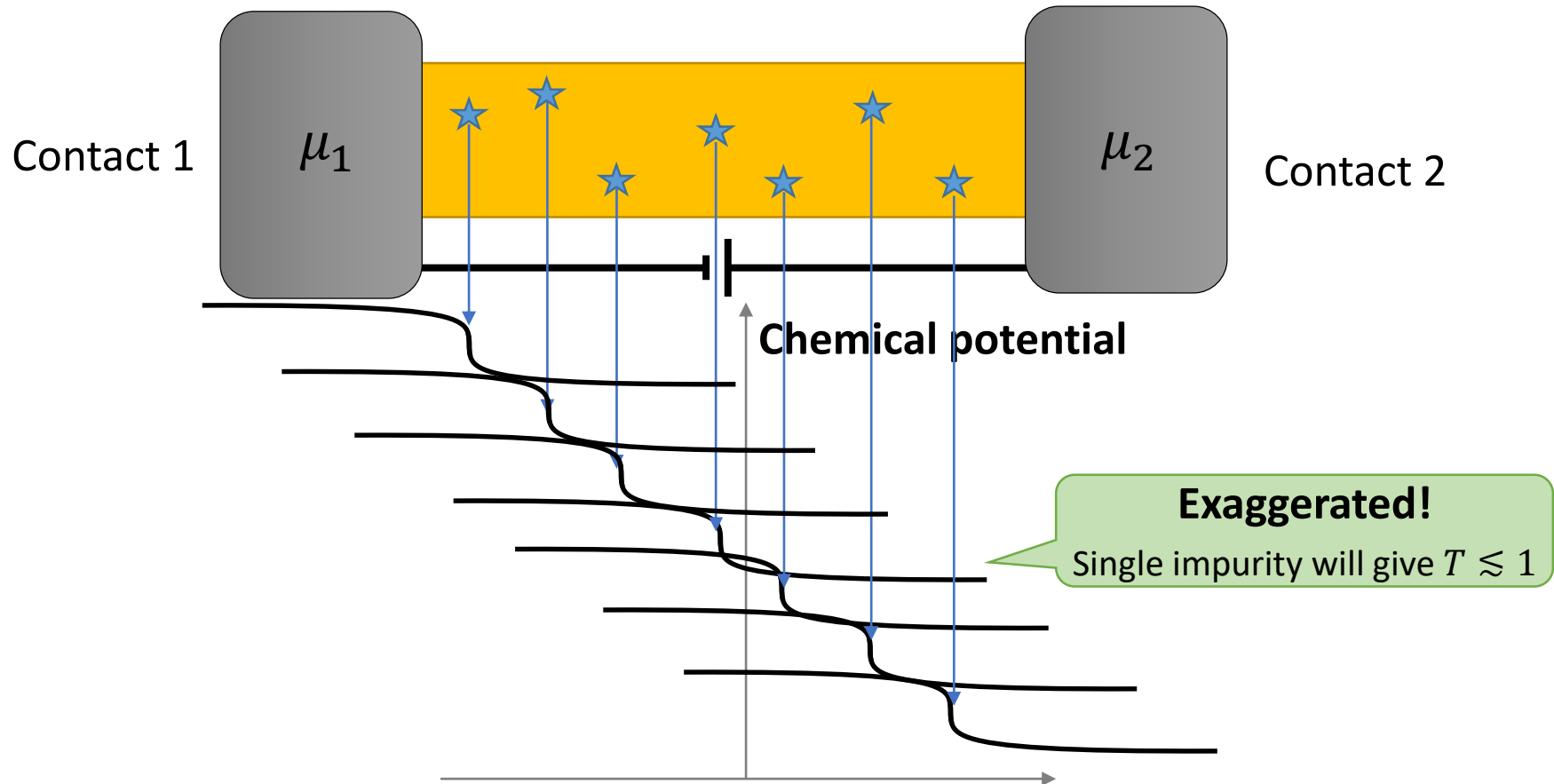
# Physics of MQT: Not perfect but ballistic conductor

- What is the electric field in the conductor?



# Physics of MQT: No perfect & diffusive conductor

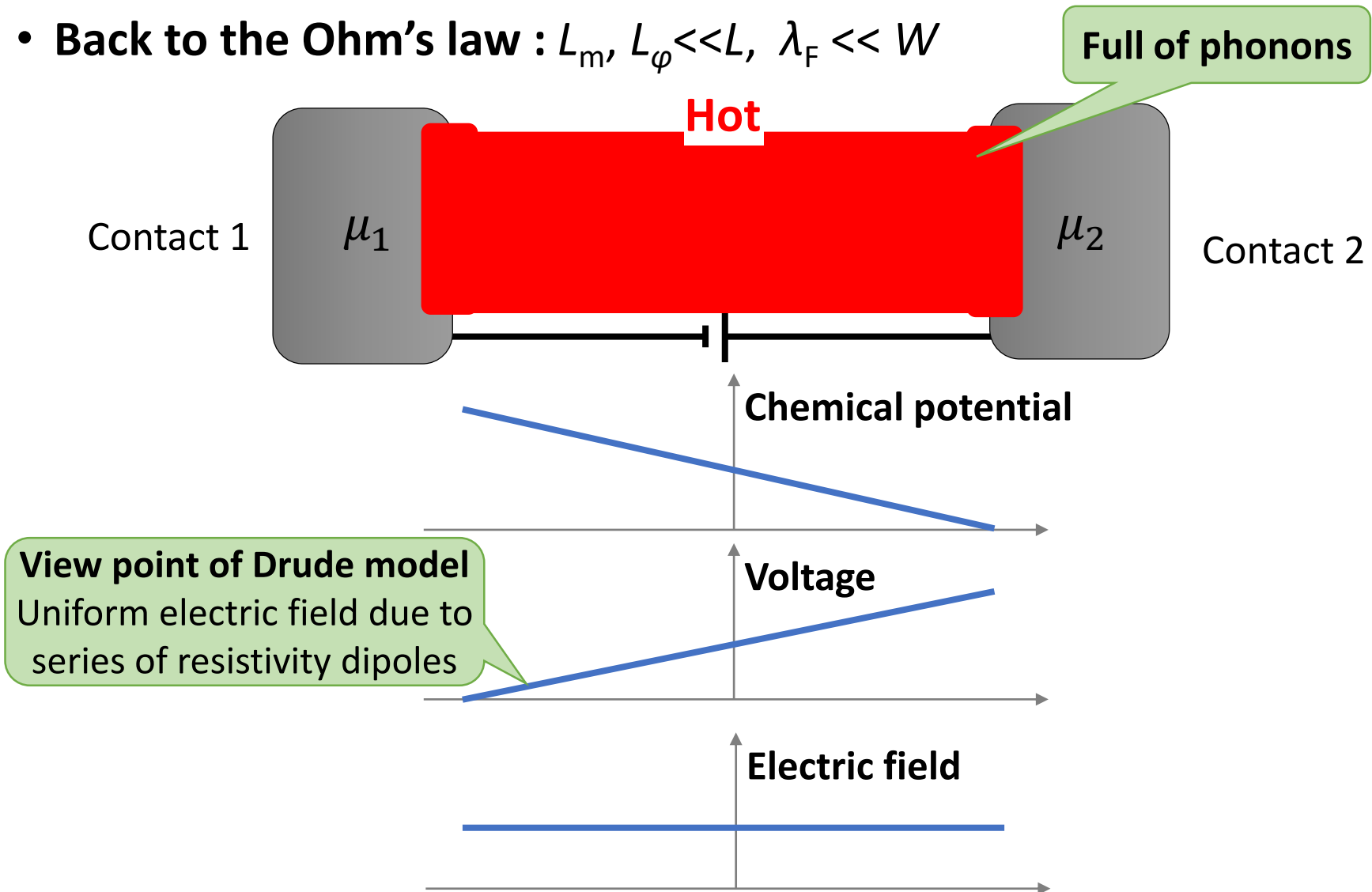
- Back to the Ohm's law :  $L_m, L_\varphi \ll L, \lambda_F \ll W$





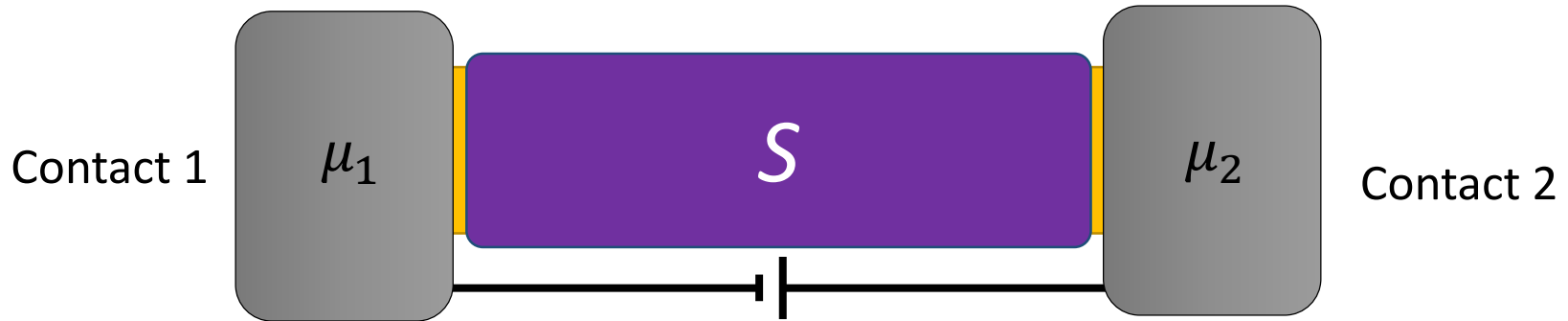
# Physics of MQT: No perfect & diffusive conductor

- Back to the Ohm's law :  $L_m, L_\phi \ll L, \lambda_F \ll W$



# Physics of MQT: Not perfect but ballistic conductor

- Back to the Ohm's law :  $L_m, L_\varphi \ll L, \lambda_F \ll W$



- Landauer formula for Ohmic regime

$$G = \frac{2e^2}{h} MT$$

$$M \sim \frac{k_F W}{\pi}$$

$$T(N) \sim \frac{L_m}{L}$$

$$G = \frac{2e^2}{h} \frac{k_F W}{\pi} \frac{L_m}{L} = \left( \frac{2e^2 k_F L_m}{h} \right) \frac{W}{L}$$

$$\sigma = \frac{2e^2 k_F}{h} \frac{\hbar k_F \tau}{2\pi m} = \frac{k_F^2}{\pi} \frac{e^2 \tau}{m} = \frac{ne^2 \tau}{m}$$

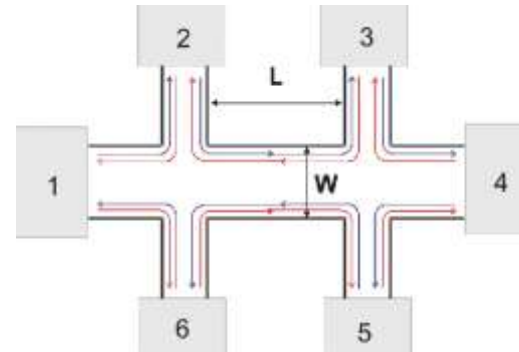
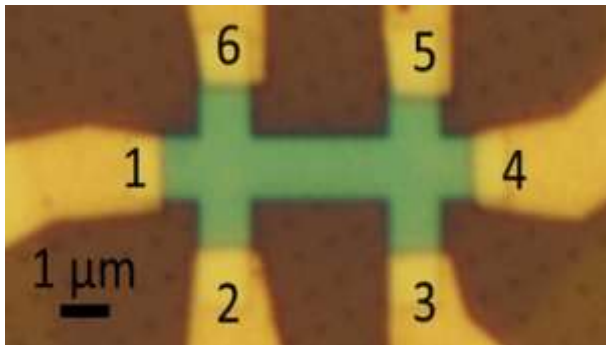
## Ohm's Law & Drude model is derived

**(Lesson)** Now we know when MQT becomes classical from a microscopic view point & How limited Drude model is.

## Landauer formalism gives another lesson:

all you need to know for transport is the S-matrix.  
(as long as it is a single particle physics)

# Physics of MQT: multi-terminal transport



- Büttiker formula: multi-terminal transport

$$I_p = \frac{2e}{h} \sum_q [T_{q \leftarrow p} \mu_p - T_{p \leftarrow q} \mu_q] = \sum_q [G_{qp} V_p - G_{pq} V_q]$$

**c.f. two-terminal case**

$$I_1 = \frac{2e}{h} (T_{21} \mu_1 - T_{12} \mu_2) = \frac{2e}{h} T_{12} (\mu_1 - \mu_2) = GV$$

$T_{21} = T_{12}$  to have  
 $I_1 = 0$  for  $\mu_1 = \mu_2$

$$G = \frac{2e^2}{h} T_{12}$$

- **Sum rule:**  $\sum_q G_{qp} = \sum_q G_{pq}$  to have  $I_p = 0$  for  $V_p = V_q = V_0$

# Physics of MQT: multi-terminal transport

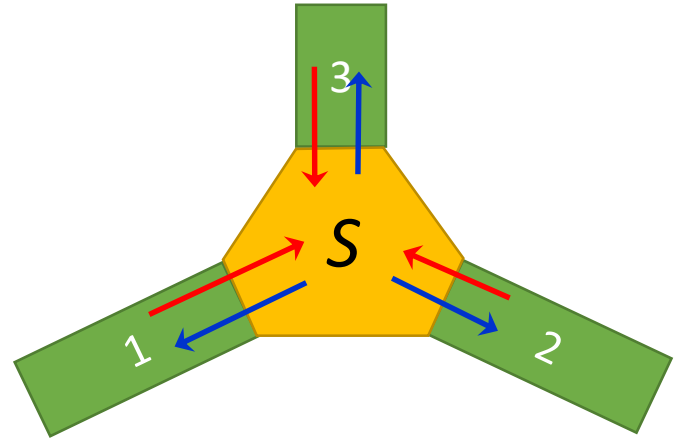
- **Three-terminal case**

$$I_1 = \frac{2e}{h} (T_{21}\mu_1 + T_{31}\mu_1 - T_{12}\mu_2 - T_{13}\mu_3)$$

$$S = \begin{pmatrix} s_{11} & s_{12} & s_{13} \\ s_{21} & s_{22} & s_{23} \\ s_{31} & s_{32} & s_{33} \end{pmatrix}$$

$$\begin{pmatrix} B_1 \\ B_2 \\ B_3 \end{pmatrix}_{\text{out}} = \begin{pmatrix} s_{11} & s_{12} & s_{13} \\ s_{21} & s_{22} & s_{23} \\ s_{31} & s_{32} & s_{33} \end{pmatrix} \begin{pmatrix} A_1 \\ A_2 \\ A_3 \end{pmatrix}_{\text{in}}$$

$$T_{21} = |s_{ab}|^2, a \text{ \& b } = ?$$



# Physics of MQT: multi-terminal transport

- Three-terminal case

$$I_1 = \frac{2e}{h} (T_{21}\mu_1 + T_{31}\mu_1 - T_{12}\mu_2 - T_{13}\mu_3)$$

$$S = \begin{pmatrix} s_{11} & s_{12} & s_{13} \\ s_{21} & s_{22} & s_{23} \\ s_{31} & s_{32} & s_{33} \end{pmatrix}$$

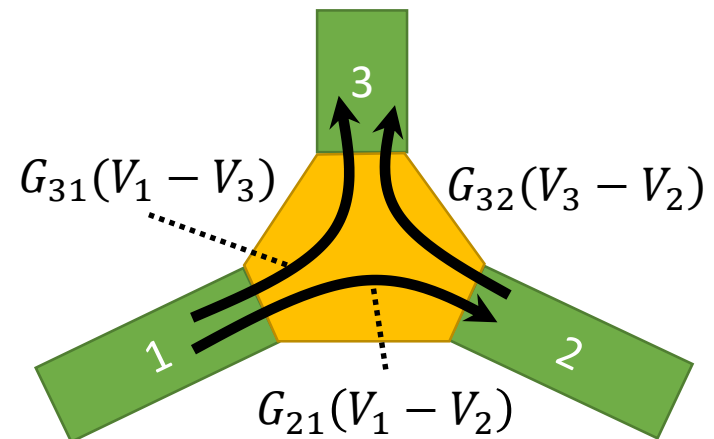
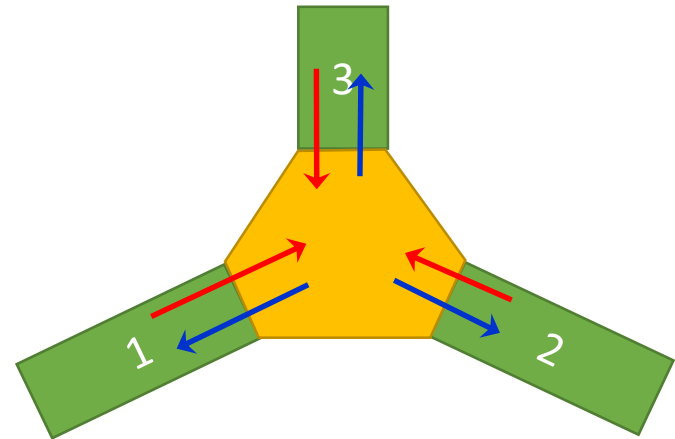
$$\begin{pmatrix} B_1 \\ B_2 \\ B_3 \end{pmatrix}_{\text{out}} = \begin{pmatrix} s_{11} & s_{12} & s_{13} \\ s_{21} & s_{22} & s_{23} \\ s_{31} & s_{32} & s_{33} \end{pmatrix} \begin{pmatrix} A_1 \\ A_2 \\ A_3 \end{pmatrix}_{\text{in}}$$

$$T_{21} = |s_{21}|^2$$

$$\begin{aligned} I_1 &= \frac{2e}{h} (T_{21}\mu_1 + T_{31}\mu_1 - T_{12}\mu_2 - T_{13}\mu_3) \\ &= G_{21}\mu_1 + G_{31}\mu_1 - G_{12}\mu_2 - G_{13}\mu_3 \\ &= G_{21}(V_1 - V_2) + G_{31}(V_1 - V_3) \end{aligned}$$

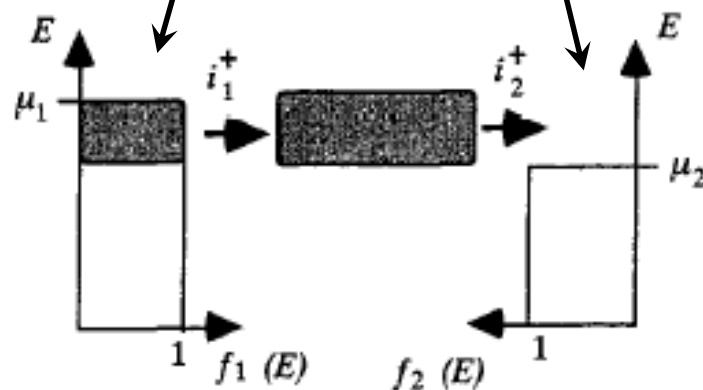
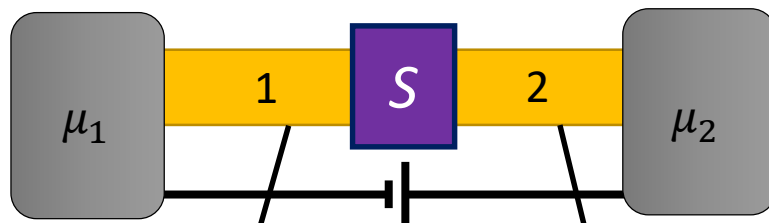
$$I_1 = -I_3 - I_2 \text{ (Kirchhoff's Law)}$$

Try!



# Physics of MQT: finite voltage bias and temperature

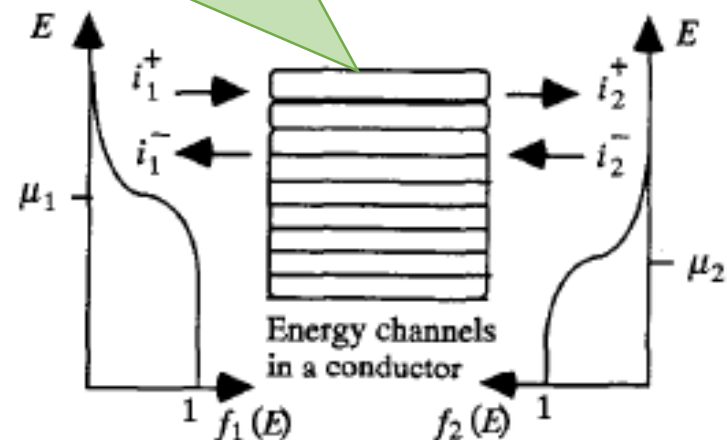
- Beyond the linear response regime: Kubo's formula is not enough
  - S-matrix, energy-dependent
  - Non-zero temperature



$$I = \frac{2e}{h} MT(\mu_1 - \mu_2) = \frac{2e}{h} MT \int [f_1(E) - f_2(E)] dE$$

$$\mapsto \frac{2e}{h} \sum_n \int T_n(E) [f_1(E) - f_2(E)] dE$$

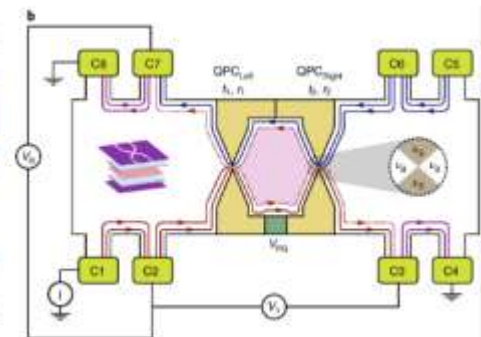
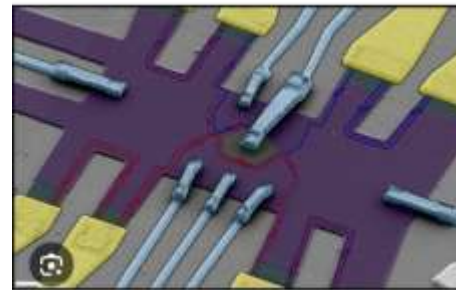
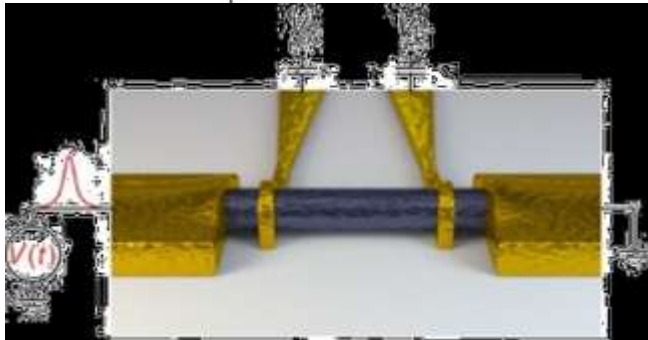
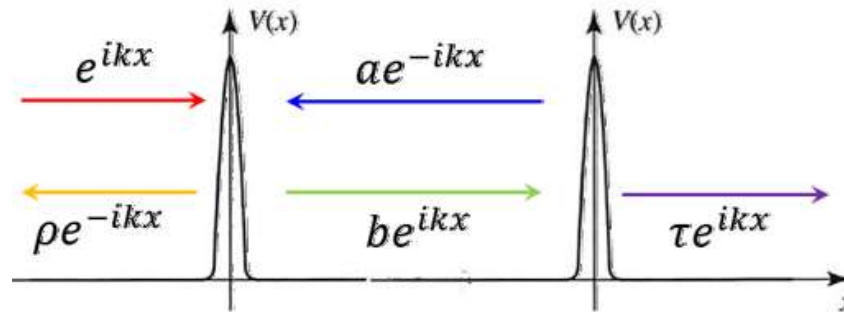
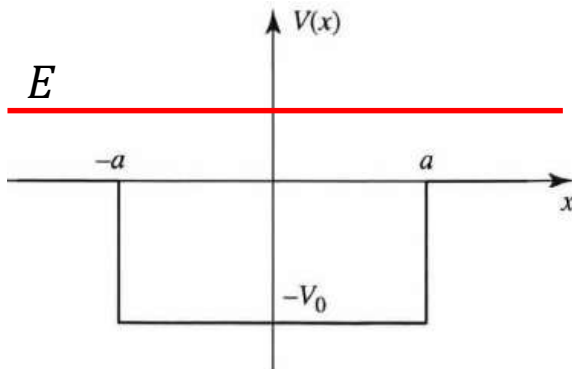
Thermoelectric transport  
can be dealt



# Application of Landauer-Büttiker formalism

- Usages of Landauer-Büttiker formalism in research (analytical)
  - **Universal physics:** precise S-matrix may not be required much
  - **Symmetry:** S-matrix can be known solely from symmetry

Resonant tunneling in MQT is universal in that particular shapes  $V(x)$  or materials do not matter



# Beyond coherent & metallic conductions

- **More about Landauer-Büttiker formalism**

- MQT is quantal: DC current =  $\langle \hat{I} \rangle$ , i.e., long-time average of current
- Current shot noise is also available [M. Büttiker, *PRB* **46**, 12485 (1992)]
- Periodically driven quantum pumps can be dealt [M. Büttiker, (1990)]

- **Beyond Landauer-Büttiker formalism: other methods for MQT**

Formalisms	Advantages	Disadvantages
<b>Landauer-Büttiker</b>	Intuitive & quick calculations. Finite voltage bias & temperature	Cannot deal with many-body physics
<b>Kubo's linear response theory</b>	Relatively easy & quick, while allowing many-body physics	Only allows physics around equilibrium states
<b>Master equation</b>	Allowing many-body physics & Nonequilibrium bias & finite temp.	Particularly useful at tunneling regime
<b>Keldysh formalism</b>	All the above	Not so easy for everyone



# Overview

- **Recap. of the last lecture: Mesoscopic Quantum Transport (MQT)**  
→ It has been exactly 1 year!
- **MQT and low-energy theory in condensed matter systems**  
→ Low-energy effective theory by  $\vec{k} \cdot \vec{p}$ -method
- **$\vec{k} \cdot \vec{p}$ -method & Mesoscopic Interactions**  
→ Mesoscopic Spin-orbit, Rashba, Zeeman interactions
- **MQT in action**  
→  $\frac{dI}{dV}$  of topological systems calculating S-matrix
- **What left beyond today's lecture**

**Mesoscopic Quantum Transport in 2 hours!**



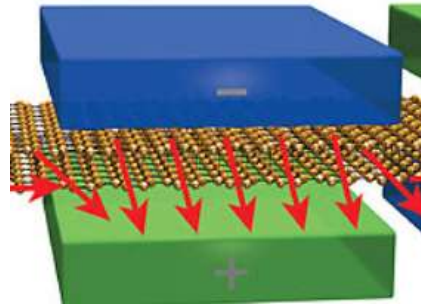
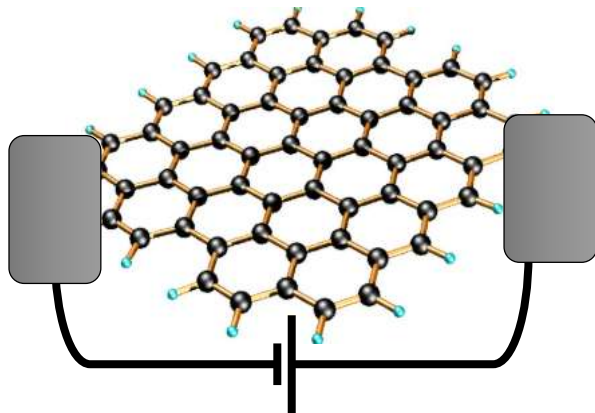
# MQT: scales matter always

- **MQT in condensed matter systems under interactions?**

→ Landauer-Büttiker formalism: S-matrix is the central quantity!

$$I = \frac{2e}{h} \int T(E) [f_1(E) - f_2(E)] dE$$

Condensed matter's  
S-matrix?



$$\begin{bmatrix} 0_{1,1} & -AX_{1,1} & -AY_{1,1} & & & \\ -AX_{1,1} & 0_{2,1} & -AX_{2,1} & & & \\ -AX_{2,1} & 0_{1,1} & -AX_{2,2} & & & \\ & -AX_{2,1} & 0_{1,1} & -AY_{1,1} & & \\ -AY_{1,1} & -AX_{1,1} & -AX_{2,1} & 0_{2,1} & -AY_{2,1} & \\ -AY_{2,1} & -AX_{2,1} & 0_{2,1} & -AX_{2,2} & -AY_{2,2} & \\ & -AY_{2,1} & -AX_{2,2} & 0_{2,2} & -AX_{3,2} & -AY_{3,2} \\ & -AY_{3,1} & -AX_{3,2} & -AX_{3,2} & 0_{2,2} & -AY_{3,2} \\ & -AY_{3,1} & -AX_{3,2} & -AY_{3,2} & -AX_{3,2} & 0_{2,2} \\ & -AY_{3,2} & -AX_{3,2} & -AY_{3,2} & -AX_{3,2} & 0_{2,2} \\ & -AY_{3,2} & -AX_{3,2} & -AY_{3,2} & -AX_{3,2} & 0_{2,2} \end{bmatrix} = \begin{bmatrix} P_{1,1} & P_{1,2} & P_{1,3} \\ P_{2,1} & P_{2,2} & P_{2,3} \\ P_{3,1} & P_{3,2} & P_{3,3} \end{bmatrix} = \begin{bmatrix} Q_{1,1} & Q_{1,2} & Q_{1,3} \\ Q_{2,1} & Q_{2,2} & Q_{2,3} \\ Q_{3,1} & Q_{3,2} & Q_{3,3} \end{bmatrix}$$



# MQT: scales matter always

- **MQT in condensed matter systems under interactions?**

→ Current at (nearly) zero temp.

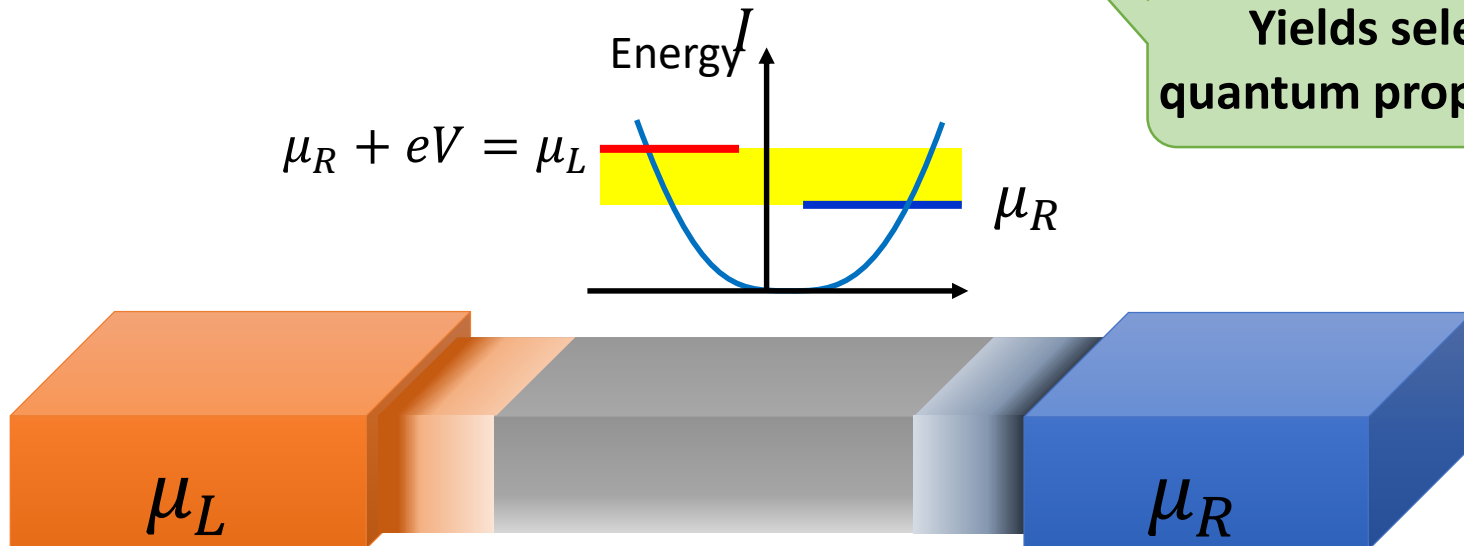
$$I = I(V) = \frac{2e}{h} \int_{\mu_R}^{\mu_L} T(E) dE$$

**S-matrix only around particular energies**

→ Differential conductance at (nearly) zero temp.

$$\frac{dI}{dV} = \frac{I(V+dV) - I(V)}{dV} = \frac{2e^2}{h} T(\mu_L)$$

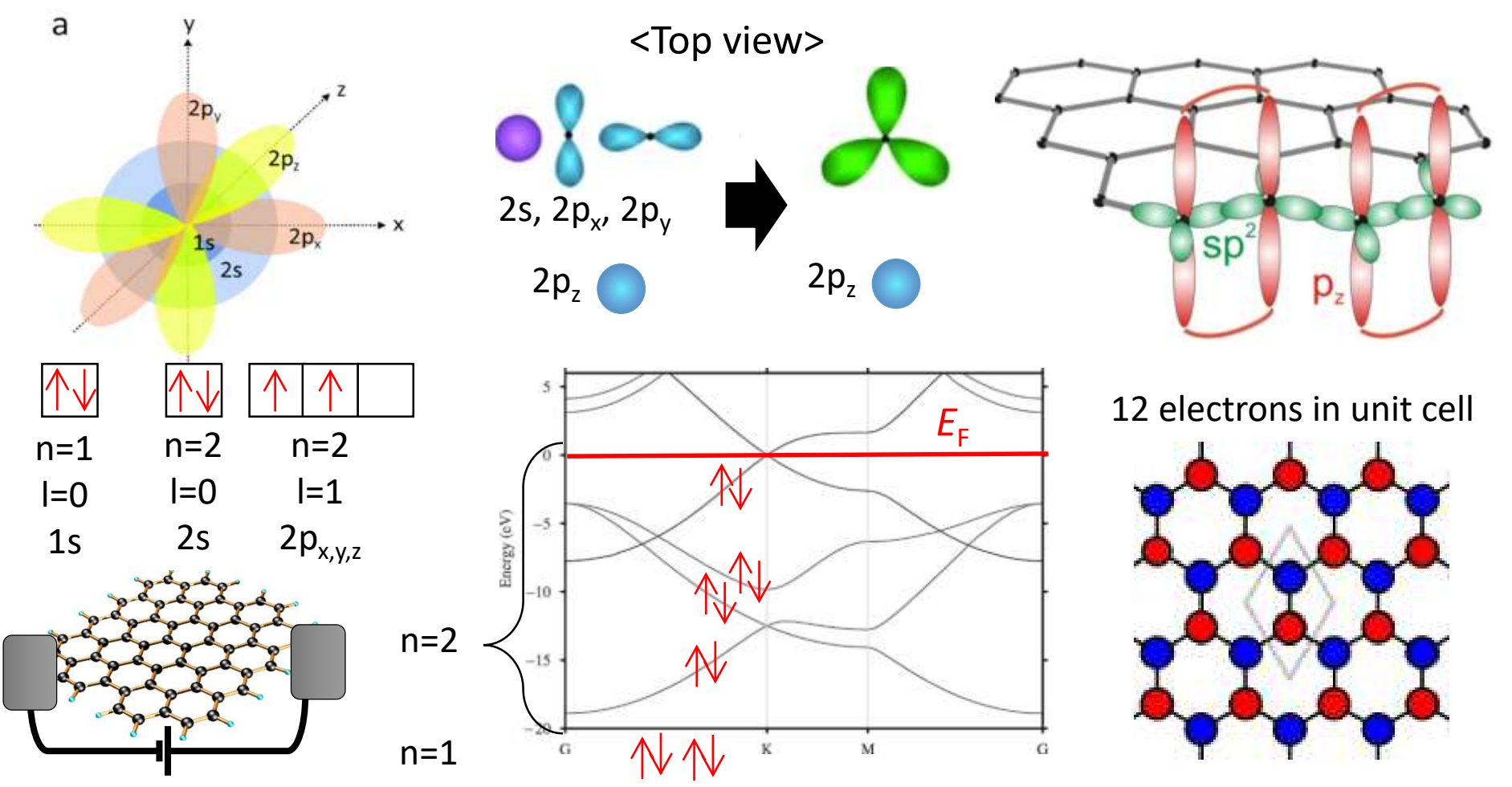
**Yields selected quantum propagations**



# MQT and low-energy theory w/ mesoscopic interactions

- Limited energy window, so what?

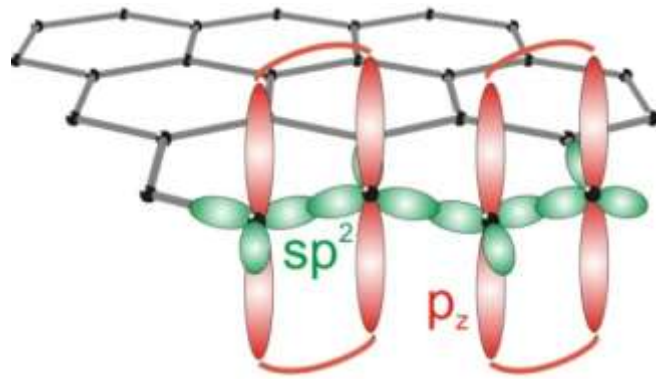
→ In the case of graphene



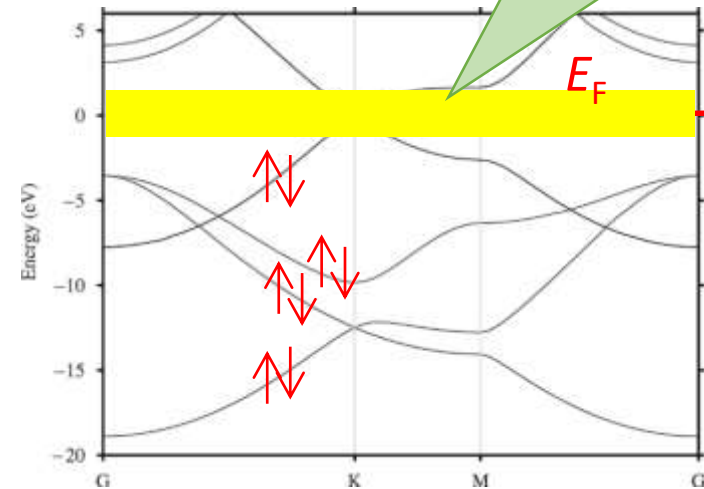
# MQT and low-energy theory w/ mesoscopic interactions

- **Limited energy window, so what?**

→ In the case of graphene

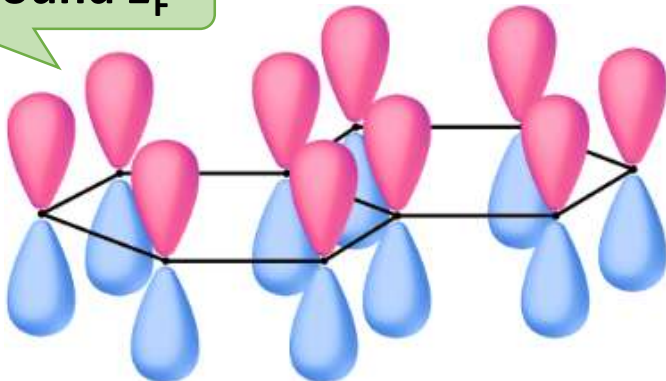


=

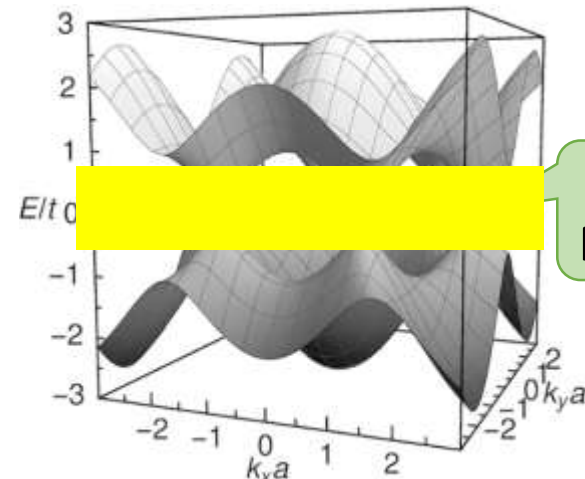


Conduction occurs around this energy

Around  $E_F$



=

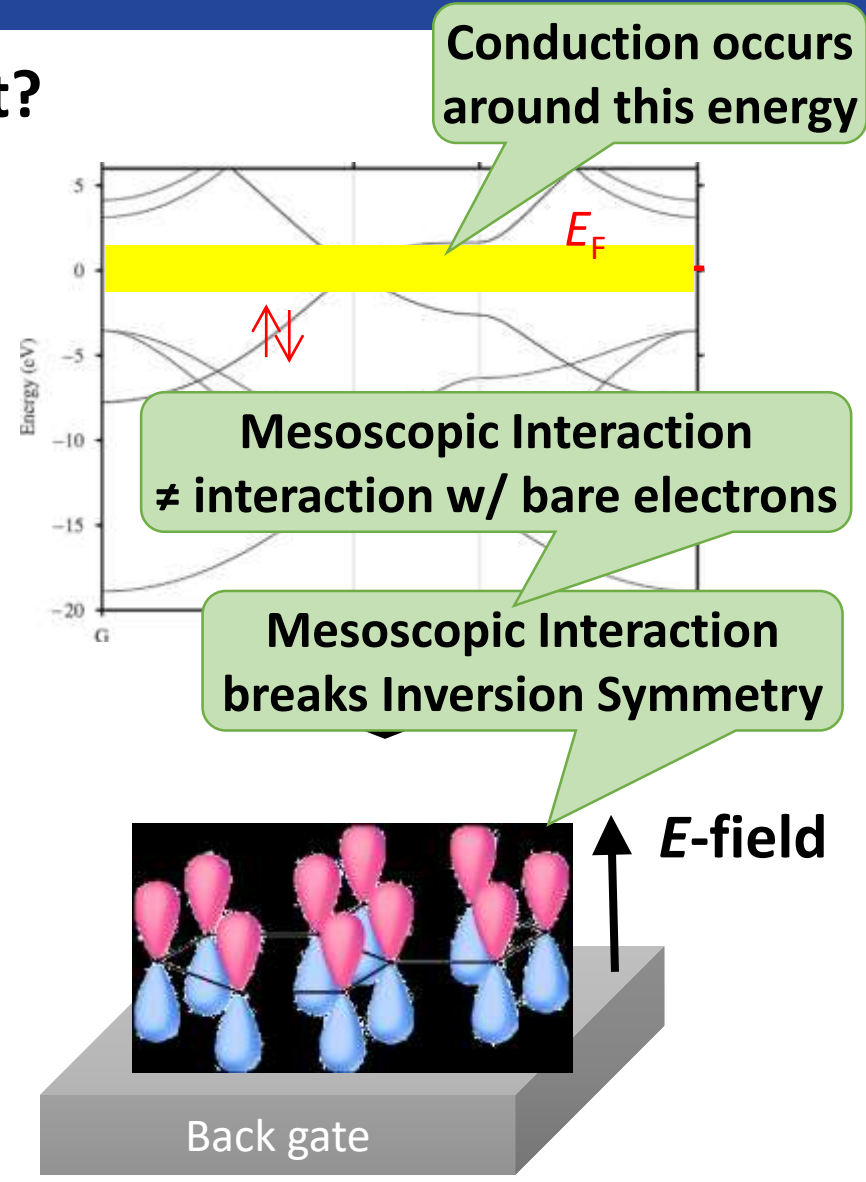
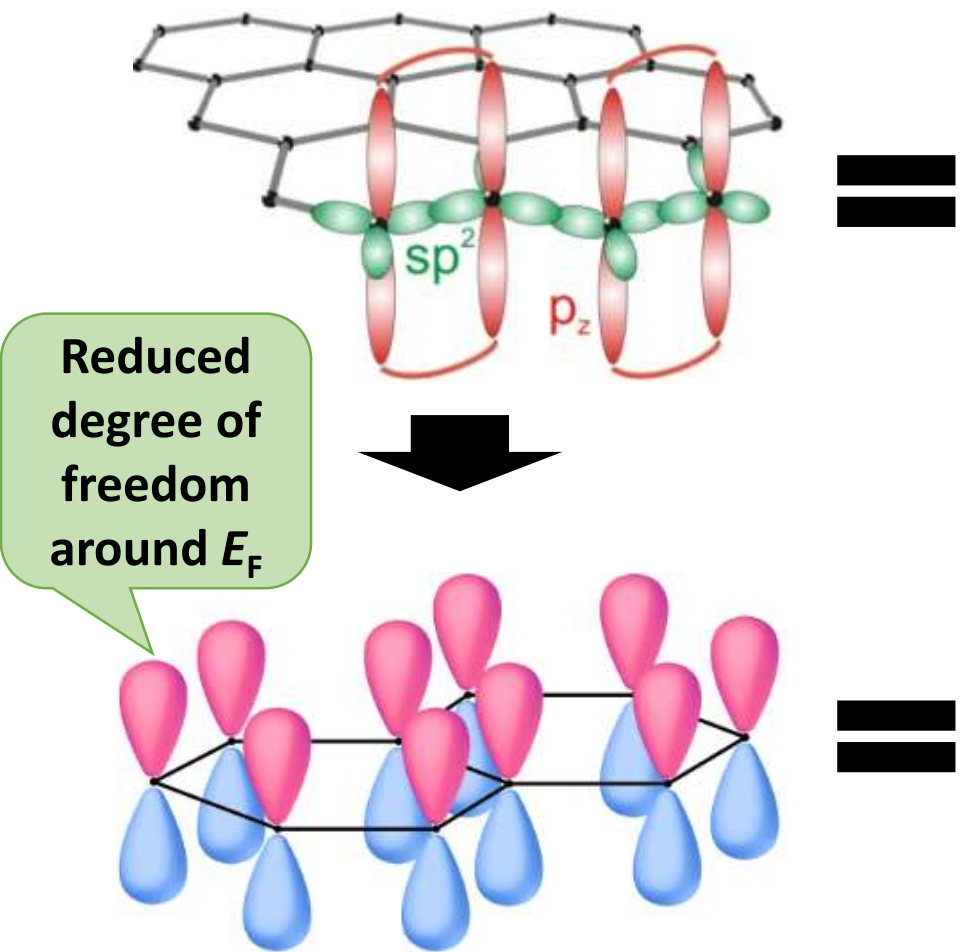


2D Dirac Fermions

# MQT and low-energy theory w/ mesoscopic interactions

- **Limited energy window, so what?**

→ In the case of graphene





# MQT and low-energy theory w/ mesoscopic interactions

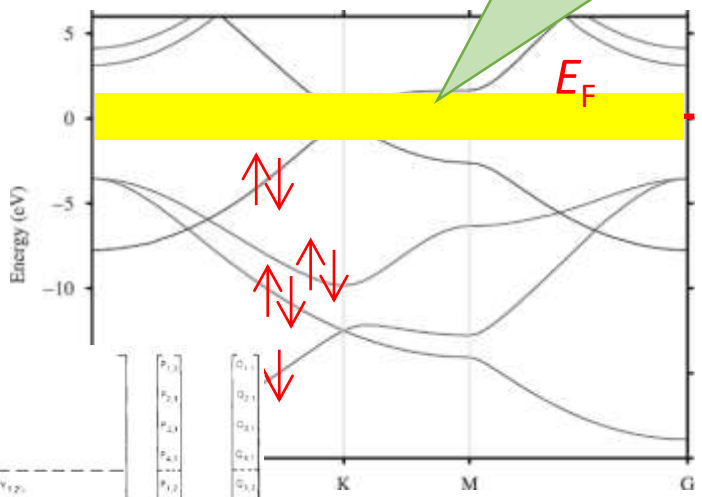
- Limited energy window, so what?

→ In the case of graphene

$\hat{H}(\vec{k})$  is a **7 by 7 matrix**

= 6 valence bands + 1 conduction band  
(without considering spins)

⊗ If we consider interactions w/ spins,  
it's doubled: 14 by 14 matrix



Conduction occurs around this energy

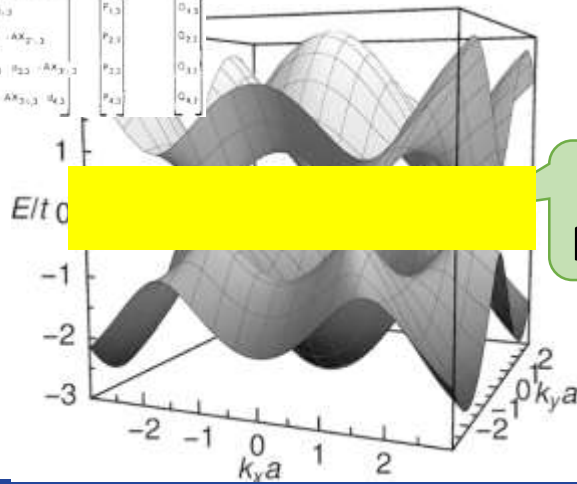
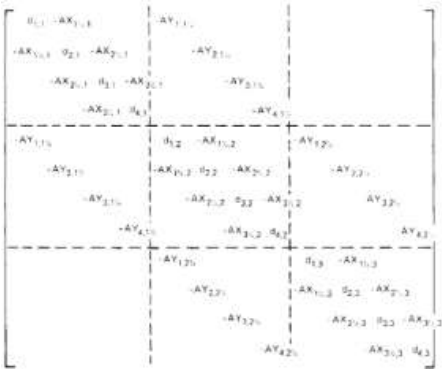


$\hat{H}(\vec{k})$  is a **2 by 2 matrix**

= 1 valence bands + 1 conduction band  
(without considering spins)

⊗ If we consider interactions w/ spins,  
it's doubled: 4 by 4 matrix

⊗  $K'$ -valley is a time-reversal partner  
of  $K$ -valley

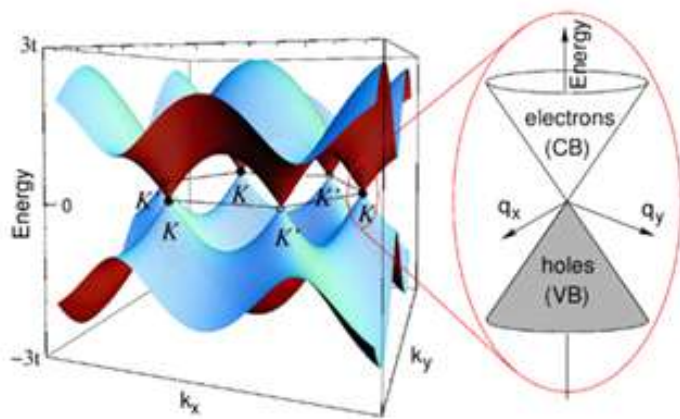


2D Dirac Fermions

# MQT and low-energy theory w/ mesoscopic interactions

- **Limited energy window, so what?**

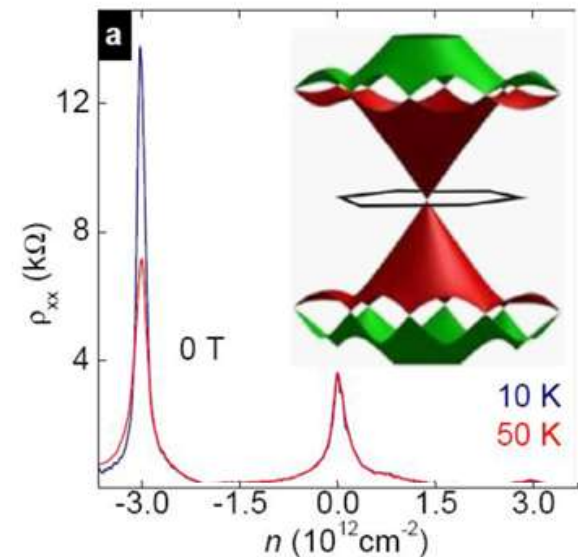
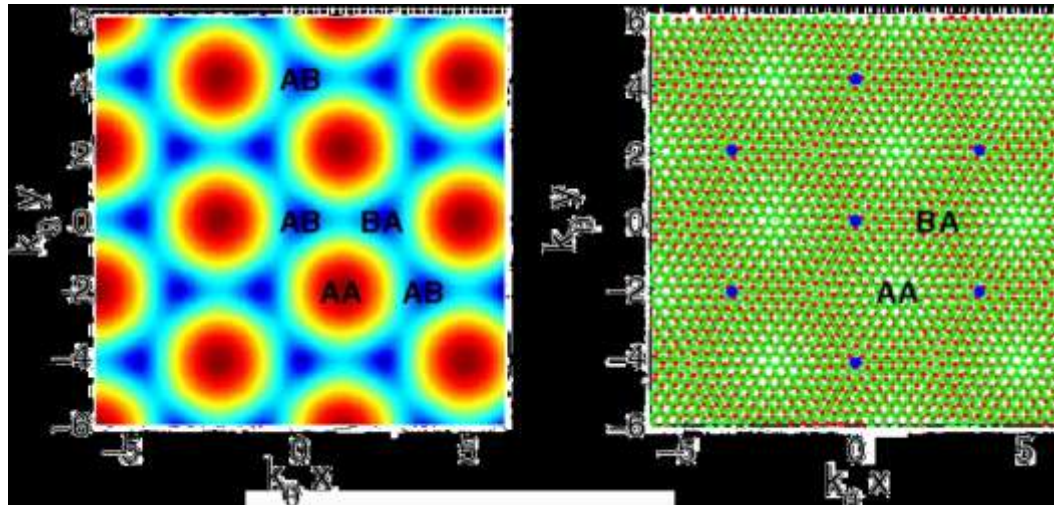
→ In the case of graphene



## 2D relativistic Dirac fermion

$$\hat{H}_{\text{eff}} = v_F \vec{p} \cdot \hat{\sigma} = v_F \begin{pmatrix} 0 & p_x - ip_y \\ p_x + ip_y & 0 \end{pmatrix}$$

Pseudospin-momentum locking

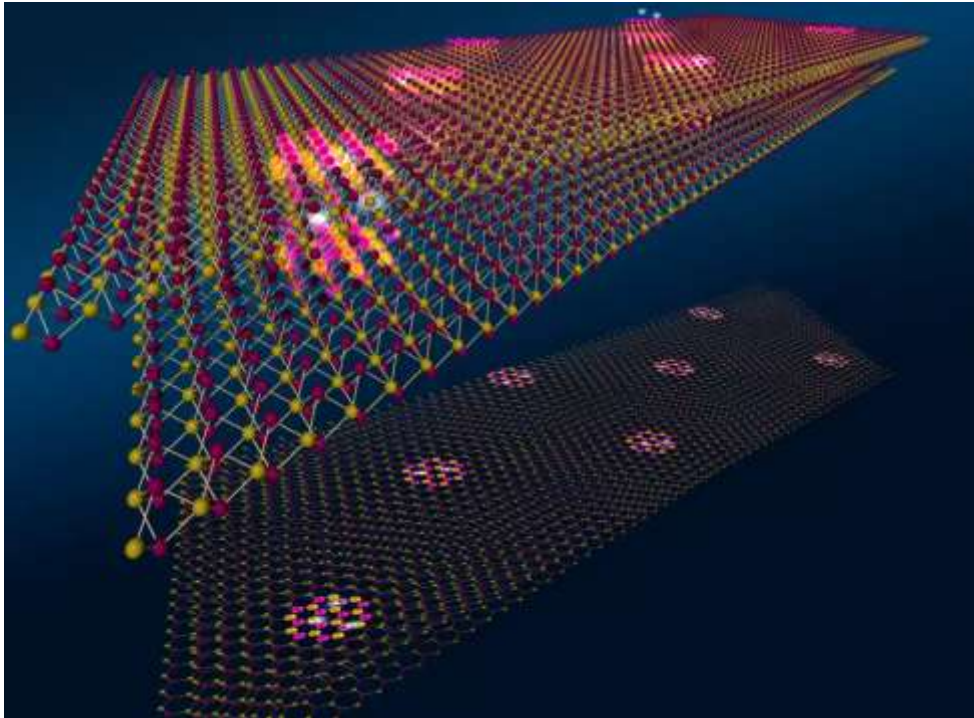




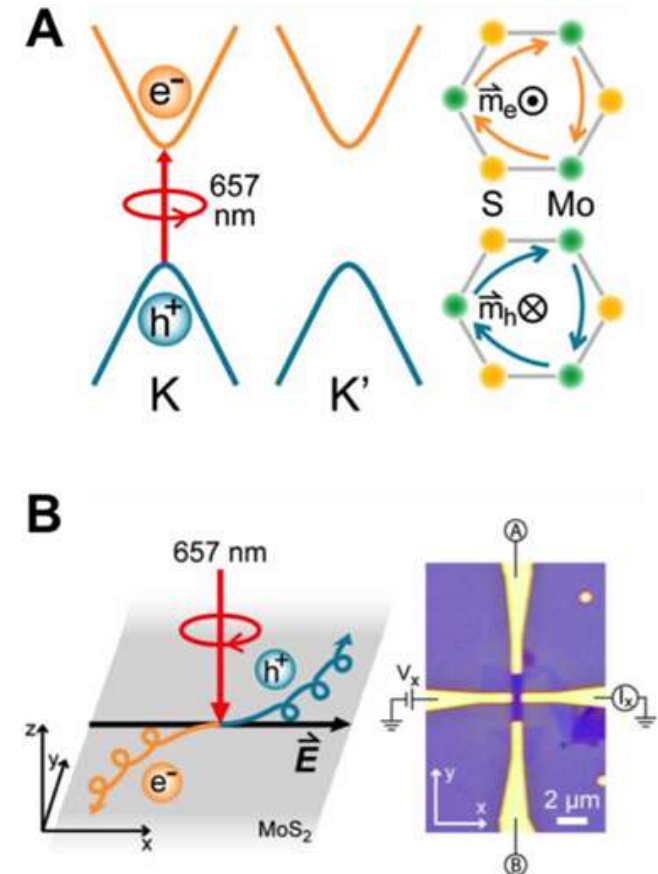
# MQT and low-energy theory w/ mesoscopic interactions

- **Limited energy window, so what?**

→ In the case of  $\text{WSe}_2$ , 2D Transition Metal Dichalcogenides (TMD)



Nature Materials **19**, 861 (2020)

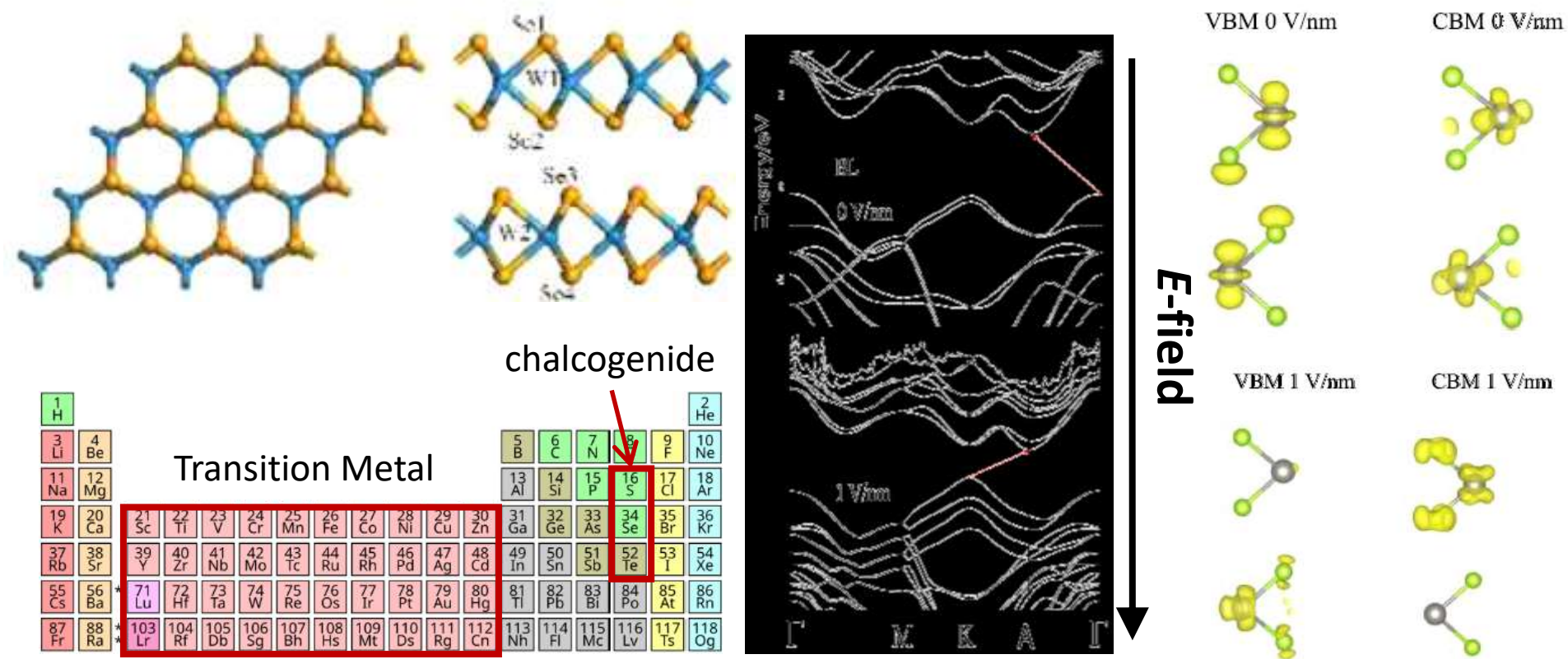


Science **344**, 1489 (2014)

# MQT and low-energy theory w/ mesoscopic interactions

- **Limited energy window, so what?**

→ In the case of  $\text{WSe}_2$ , 2D Transition Metal Dichalcogenides (TMD)



Journal of Applied Physics **117**, 084310 (2015)

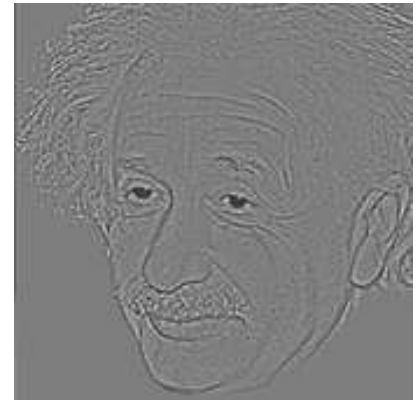
# $\vec{k} \cdot \vec{p}$ -method in action: formalism

- **Low-energy effective Hamiltonian:  $\vec{k} \cdot \vec{p}$ -method**

→ How does a system look around a particular momentum



**Around large  $k$   
this looks**



**Around small  $k$   
this looks**



# $\vec{k} \cdot \vec{p}$ -method in action: formalism

- **Low-energy effective Hamiltonian:**  $\vec{k} \cdot \vec{p}$ -method

→ How does a system look around a particular momentum  $\vec{k}$

→ There will be eigenstates  $|n\vec{k}\rangle$  of the full Hamiltonian  $\hat{H}$

$$\hat{H}(\vec{k}) |n\vec{k}\rangle = E_n(\vec{k}) |n\vec{k}\rangle$$

→ Select subspace of the full Hilbert space with  $n$ 's such that

$E_n(\vec{k})$  is around Fermi energy. Let's say those are  $n=1,2$

→ Matrix representation of the low-energy Hamiltonian around  $E_F$

$$\hat{H}_{\text{eff}}(\vec{p}) = \begin{pmatrix} \langle 1\vec{k} | \hat{H}(\vec{k} + \vec{p}) | 1\vec{k} \rangle & \langle 1\vec{k} | \hat{H}(\vec{k} + \vec{p}) | 2\vec{k} \rangle \\ \langle 2\vec{k} | \hat{H}(\vec{k} + \vec{p}) | 1\vec{k} \rangle & \langle 2\vec{k} | \hat{H}(\vec{k} + \vec{p}) | 2\vec{k} \rangle \end{pmatrix}$$

You can choose  $n$ 's as many as you want

# $\vec{k} \cdot \vec{p}$ -method in action: formalism

- **Low-energy effective Hamiltonian:  $\vec{k} \cdot \vec{p}$ -method**

$$\hat{H}_{\text{eff}}(\vec{p}) = \begin{pmatrix} \langle 1\vec{k} | \hat{H}(\vec{k} + \vec{p}) | 1\vec{k} \rangle & \langle 1\vec{k} | \hat{H}(\vec{k} + \vec{p}) | 2\vec{k} \rangle \\ \langle 2\vec{k} | \hat{H}(\vec{k} + \vec{p}) | 1\vec{k} \rangle & \langle 2\vec{k} | \hat{H}(\vec{k} + \vec{p}) | 2\vec{k} \rangle \end{pmatrix}$$

- **Philosophy behind  $\vec{k} \cdot \vec{p}$ -method**

→ Put  $\vec{p} = 0$

$$\hat{H}_{\text{eff}}(0) = \begin{pmatrix} \langle 1\vec{k} | \hat{H}(\vec{k}) | 1\vec{k} \rangle & \langle 1\vec{k} | \hat{H}(\vec{k}) | 2\vec{k} \rangle \\ \langle 2\vec{k} | \hat{H}(\vec{k}) | 1\vec{k} \rangle & \langle 2\vec{k} | \hat{H}(\vec{k}) | 2\vec{k} \rangle \end{pmatrix} = \begin{pmatrix} E_{1\vec{k}} & 0 \\ 0 & E_{2\vec{k}} \end{pmatrix}$$

Exact

→ If  $\vec{p}$  is small,

$$|n, \vec{k} + \vec{p}\rangle \approx |n, \vec{k}\rangle$$

1<sup>st</sup> order Perturbation  
(2<sup>nd</sup> order is often used)

→ Accordingly,

$$\hat{H}_{\text{eff}}(\vec{p}) = \begin{pmatrix} \langle 1\vec{k} | \hat{H}(\vec{k} + \vec{p}) | 1\vec{k} \rangle & \langle 1\vec{k} | \hat{H}(\vec{k} + \vec{p}) | 2\vec{k} \rangle \\ \langle 2\vec{k} | \hat{H}(\vec{k} + \vec{p}) | 1\vec{k} \rangle & \langle 2\vec{k} | \hat{H}(\vec{k} + \vec{p}) | 2\vec{k} \rangle \end{pmatrix}$$



# $\vec{k} \cdot \vec{p}$ -method in action: Low-energy effective $H$

## • 2D Transition Metal Dichalcogenides

→ PRL **108**, 196802 (2012)

Coupled Spin and Valley Physics in Monolayers of MoS<sub>2</sub> and Other Group-VI Dichalcogenides

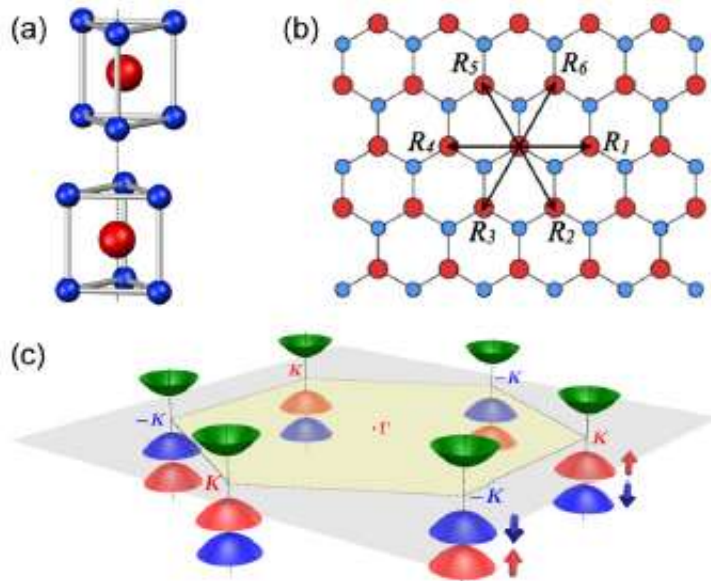
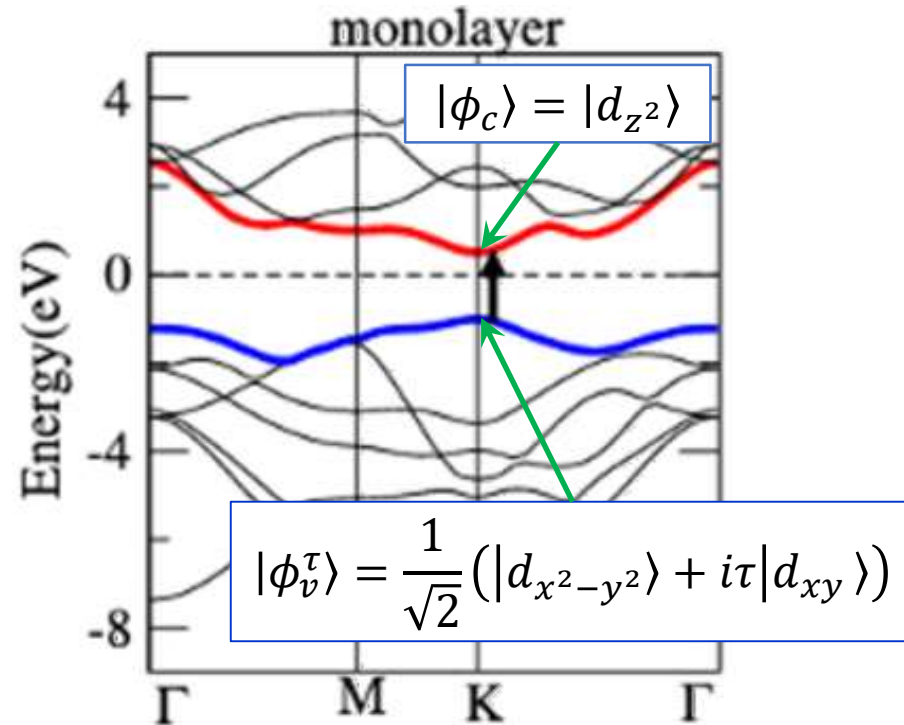


FIG. 1 (color online). (a) The unit cell of bulk 2H-MoS<sub>2</sub>, which has the inversion center located in the middle plane. It contains two unit cells of MoS<sub>2</sub> monolayers, which lacks an inversion center. (b) Top view of the MoS<sub>2</sub> monolayer.  $R_i$  are the vectors connecting nearest Mo atoms. (c) Schematic drawing of the band structure at the band edges located at the  $K$  points.



Journal of Applied Physics **117**, 084310 (2015)

# $\vec{k} \cdot \vec{p}$ -method in action: Low-energy effective $H$

## • 2D Transition Metal Dichalcogenides

→ PRL **108**, 196802 (2012)

Coupled Spin and Valley Physics in Monolayers of MoS<sub>2</sub> and Other Group-VI Dichalcogenides

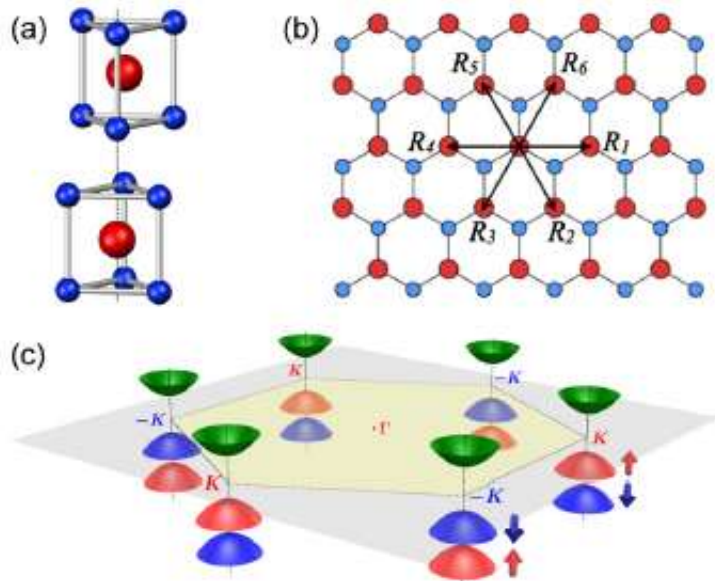


FIG. 1 (color online). (a) The unit cell of bulk 2H-MoS<sub>2</sub>, which has the inversion center located in the middle plane. It contains two unit cells of MoS<sub>2</sub> monolayers, which lacks an inversion center. (b) Top view of the MoS<sub>2</sub> monolayer.  $R_i$  are the vectors connecting nearest Mo atoms. (c) Schematic drawing of the band structure at the band edges located at the  $K$  points.

shown in Fig. 1(c). The group of the wave vector at the band edges ( $K$ ) is  $C_{3h}$  and the symmetry adapted basis functions are

$$|\phi_c\rangle = |d_{z^2}\rangle, \quad |\phi_v^\tau\rangle = \frac{1}{\sqrt{2}}(|d_{x^2-y^2}\rangle + i\tau|d_{xy}\rangle), \quad (1)$$

$\tau = 1(-1)$  for  $K(K')$ -valley To first order in  $k$ , the  $C_{3h}$  symmetry dictates that the two-band  $k \cdot p$  Hamiltonian has the form

$$\hat{H}_0 = at(\tau \hat{\sigma}_x + \hat{\sigma}_y) + \frac{\Delta}{2} \hat{\sigma}_z, \quad (2)$$

state splits. Approximating the SOC by the intra-atomic contribution  $L \cdot S$ , we find the total Hamiltonian given by

$$\hat{H} = at(\tau k_x \hat{\sigma}_x + k_y \hat{\sigma}_y) + \frac{\Delta}{2} \hat{\sigma}_z \quad (3)$$

Mesoscopic interaction

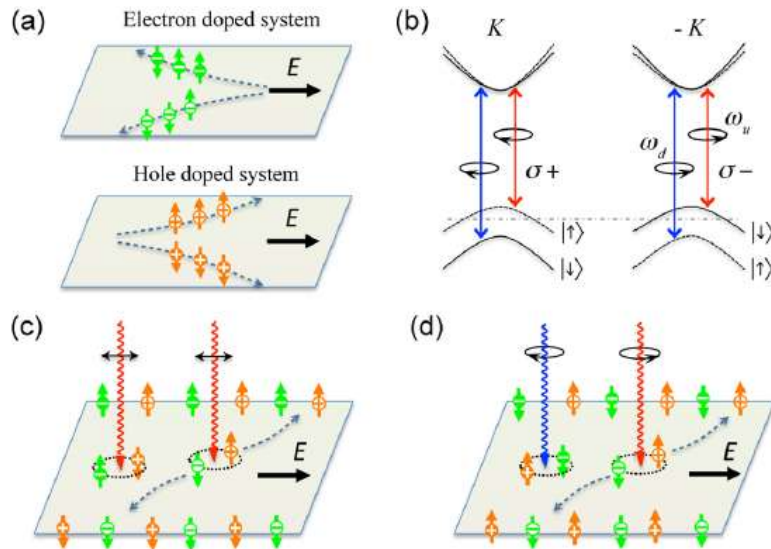
where  $2\lambda$  is the spin splitting at the valence band top caused by the SOC and  $\hat{s}_z$  is the Pauli matrix for spin.

# $\vec{k} \cdot \vec{p}$ -method in action: Low-energy effective $H$

## • 2D Transition Metal Dichalcogenides

→ PRL **108**, 196802 (2012)

Coupled Spin and Valley Physics in Monolayers of MoS2 and Other Group-VI Dichalcogenides



$$\Omega_c(k) = -\tau \frac{2a^2 t^2 \Delta'}{[\Delta'^2 + 4a^2 t^2 k^2]^{3/2}}.$$

shown in Fig. 1(c). The group of the wave vector at the band edges ( $K$ ) is  $C_{3h}$  and the symmetry adapted basis functions are

$$|\phi_c\rangle = |d_{z^2}\rangle, \quad |\phi_v^\tau\rangle = \frac{1}{\sqrt{2}}(|d_{x^2-y^2}\rangle + i\tau|d_{xy}\rangle), \quad (1)$$

$\tau = 1(-1)$  for  $K(K')$ -valley To first order in  $k$ , the  $C_{3h}$  symmetry dictates that the two-band  $k \cdot p$  Hamiltonian has the form

$$\hat{H}_0 = at(\tau \hat{\sigma}_x + \hat{\sigma}_y) + \frac{\Delta}{2} \hat{\sigma}_z, \quad (2)$$

state splits. Approximating the SOC by the intra-atomic contribution  $\mathbf{L} \cdot \mathbf{S}$ , we find the total Hamiltonian given by

$$\hat{H} = at(\tau k_x \hat{\sigma}_x + k_y \hat{\sigma}_y) + \frac{\Delta}{2} \hat{\sigma}_z \quad (3)$$

Mesoscopic interaction

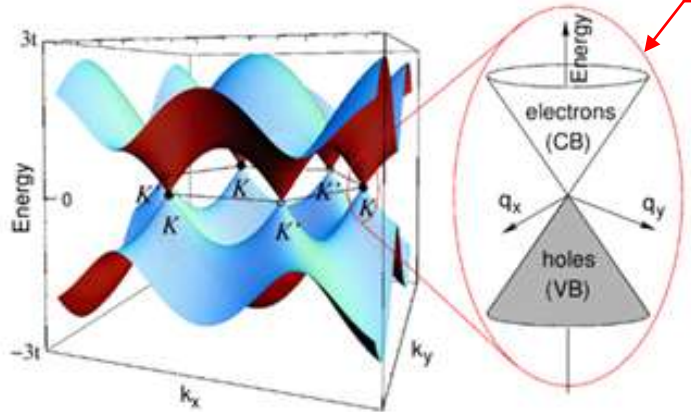
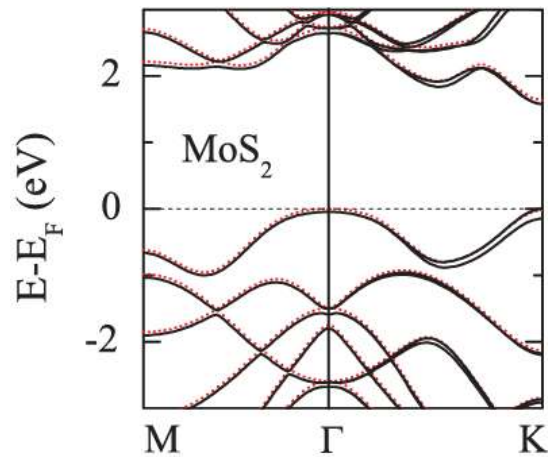
where  $2\lambda$  is the spin splitting at the valence band top caused by the SOC and  $\hat{s}_z$  is the Pauli matrix for spin.



# $\vec{k} \cdot \vec{p}$ -method in action: Low-energy effective $H$

## • 2D Transition Metal Dichalcogenides

→ PRL **108**, 196802 (2012)



shown in Fig. 1(c). The group of the wave vector at the band edges ( $K$ ) is  $C_{3h}$  and the symmetry adapted basis functions are

$$|\phi_c\rangle = |d_{z^2}\rangle, \quad |\phi_v^\tau\rangle = \frac{1}{\sqrt{2}}(|d_{x^2-y^2}\rangle + i\tau|d_{xy}\rangle), \quad (1)$$

$\tau = 1(-1)$  for  $K(K')$ -valley To first order in  $k$ , the  $C_{3h}$  symmetry dictates that the two-band  $k \cdot p$  Hamiltonian has the form

**Graphene**  
 $\hat{H}_{\text{eff}} = v_F \vec{p} \cdot \hat{\sigma}$

$$\hat{H}_{\text{eff}} = v_F \vec{p} \cdot \hat{\sigma} \quad (2)$$

state splits. Approximating the SOC by the intra-atomic contribution  $L \cdot S$ , we find the total Hamiltonian given by

$$\hat{H} = at(\tau k_x \hat{\sigma}_x + k_y \hat{\sigma}_y) + \frac{\Delta}{2} \hat{\sigma}_z - \lambda \tau \frac{\hat{\sigma}_z - 1}{2} \hat{s}_z, \quad (3)$$

where  $2\lambda$  is the spin splitting at the valence band top caused by the SOC and  $\hat{s}_z$  is the Pauli matrix for spin.

# $\vec{k} \cdot \vec{p}$ -method in action: Low-energy effective $H$

## • 2D Transition Metal Dichalcogenides

→ PRL **108**, 196802 (2012)

### Counting Symmetry

e.g., Time-reversal symmetry

$$\hat{\Theta} = i\hat{\sigma}_y K? [\hat{H}_0, \hat{\Theta}] = 0?$$

$$\hat{\Theta}^{-1} \hat{H}_0^\tau \hat{\Theta} = \hat{\sigma}_y (\hat{H}_0^\tau)^* \hat{\sigma}_y = \hat{H}_0^{-\tau}?$$

where  $\hat{\Theta}^{-1} = -i\hat{\sigma}_y K$ .

$$\hat{\sigma}_y (\hat{H}_0^\tau)^* \hat{\sigma}_y =$$

$$\hat{\sigma}_y \left[ at(-i\tau\partial_x\hat{\sigma}_x - i\partial_y\hat{\sigma}_y) + \frac{\Delta}{2}\hat{\sigma}_z \right]^* \hat{\sigma}_y$$

$$= \hat{\sigma}_y \left[ at(i\tau\partial_x\hat{\sigma}_x - i\partial_y\hat{\sigma}_y) + \frac{\Delta}{2}\hat{\sigma}_z \right] \hat{\sigma}_y$$

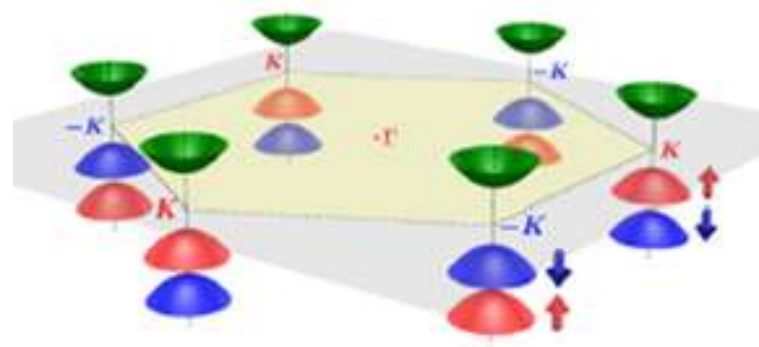
$$= at(-i\tau\partial_x\hat{\sigma}_x - i\partial_y\hat{\sigma}_y) - \frac{\Delta}{2}\hat{\sigma}_z \neq \hat{H}_0^{-\tau}$$

shown in Fig. 1(c). The group of the wave vector at the band edges ( $K$ ) is  $C_{3h}$  and the symmetry adapted basis functions are

$$|\phi_c\rangle = |d_{z^2}\rangle, \quad |\phi_v^\tau\rangle = \frac{1}{\sqrt{2}}(|d_{x^2-y^2}\rangle + i\tau|d_{xy}\rangle), \quad (1)$$

$\tau = 1(-1)$  for  $K(K')$ -valley To first order in  $k$ , the  $C_{3h}$  symmetry dictates that the two-band  $k \cdot p$  Hamiltonian has the form

$$\hat{H}_0 = at(\tau k_x \hat{\sigma}_x + k_y \hat{\sigma}_y) + \frac{\Delta}{2} \hat{\sigma}_z, \quad (2)$$



# $\vec{k} \cdot \vec{p}$ -method in action: Low-energy effective $H$

## • 2D Transition Metal Dichalcogenides

→ PRL **108**, 196802 (2012)

### Counting Symmetry

e.g., Time-reversal symmetry  $\hat{\Theta} = i\hat{\sigma}_y K$  is not so correct,  $\hat{\sigma}$ 's are about orbitals. Hence,  $\hat{\Theta} \mapsto K$  with  $\hat{\Theta}^2 = 1$ . See

$$\hat{\Theta}|\phi_v^\tau\rangle = |\phi_v^{-\tau}\rangle.$$

Now,

$$\begin{aligned}\hat{\Theta}^{-1}\hat{H}_0^\tau\hat{\Theta} &= \left[at(-i\tau\partial_x\hat{\sigma}_x - i\partial_y\hat{\sigma}_y) + \frac{\Delta}{2}\hat{\sigma}_z\right]^* \\ &= at(-i(-\tau)\partial_x\hat{\sigma}_x - i\partial_y\hat{\sigma}_y) + \frac{\Delta}{2}\hat{\sigma}_z \\ &= \hat{H}_0^{-\tau}\end{aligned}$$

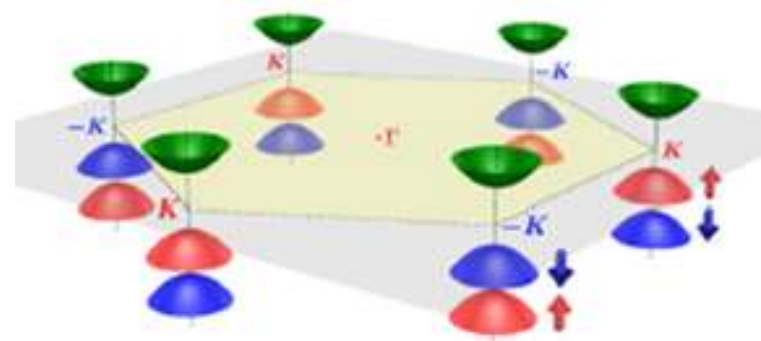
**Time-reversal of low-energy  $H$  of  $K$ -valley is that of  $K'$ -valley**

shown in Fig. 1(c). The group of the wave vector at the band edges ( $K$ ) is  $C_{3h}$  and the symmetry adapted basis functions are

$$|\phi_c\rangle = |d_{z^2}\rangle, \quad |\phi_v^\tau\rangle = \frac{1}{\sqrt{2}}(|d_{x^2-y^2}\rangle + i\tau|d_{xy}\rangle), \quad (1)$$

$\tau = 1(-1)$  for  $K(K')$ -valley To first order in  $k$ , the  $C_{3h}$  symmetry dictates that the two-band  $k \cdot p$  Hamiltonian has the form

$$\hat{H}_0 = at(\tau k_x \hat{\sigma}_x + k_y \hat{\sigma}_y) + \frac{\Delta}{2} \hat{\sigma}_z, \quad (2)$$



# $\vec{k} \cdot \vec{p}$ -method in action: Low-energy effective $H$

## • 2D Transition Metal Dichalcogenides

→ PRL **108**, 196802 (2012)

### Counting Symmetry

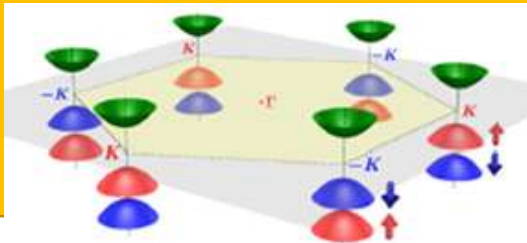
e.g., Time-reversal symmetry

Now you see  $\hat{\Theta} = i\hat{s}_y K$  is correct,

$\hat{s}$ 's are about spins. Check

$$\begin{aligned}\hat{\Theta}^{-1} \hat{H}^{\tau} \hat{\Theta} &= \hat{s}_y \left[ \hat{H}_0^{\tau} - \lambda \tau \frac{\hat{\sigma}_z - 1}{2} \hat{s}_z \right]^* \hat{s}_y \\ &= \hat{H}_0^{-\tau} + \hat{s}_y \left( -\lambda \tau \frac{\hat{\sigma}_z - 1}{2} \hat{s}_z \right) \hat{s}_y \\ &= \hat{H}_0^{-\tau} - \lambda (-\tau) \frac{\hat{\sigma}_z - 1}{2} \hat{s}_z = \hat{H}^{-\tau}\end{aligned}$$

**Time-reversal of low-energy  $H$  of  $K$ -valley is that of  $K'$ -valley**



shown in Fig. 1(c). The group of the wave vector at the band edges ( $K$ ) is  $C_{3h}$  and the symmetry adapted basis functions are

$$|\phi_c\rangle = |d_{z^2}\rangle, \quad |\phi_v^{\tau}\rangle = \frac{1}{\sqrt{2}}(|d_{x^2-y^2}\rangle + i\tau|d_{xy}\rangle), \quad (1)$$

$\tau = 1(-1)$  for  $K(K')$ -valley To first order in  $k$ , the  $C_{3h}$  symmetry dictates that the two-band  $k \cdot p$  Hamiltonian has the form

$$\hat{H}_0 = at(\tau k_x \hat{\sigma}_x + k_y \hat{\sigma}_y) + \frac{\Delta}{2} \hat{\sigma}_z, \quad (2)$$

state splits. Approximating the SOC by the intra-atomic contribution  $L \cdot S$ , we find the total Hamiltonian given by

$$\hat{H} = at(\tau k_x \hat{\sigma}_x + k_y \hat{\sigma}_y) + \frac{\Delta}{2} \hat{\sigma}_z - \lambda \tau \frac{\hat{\sigma}_z - 1}{2} \hat{s}_z, \quad (3)$$

where  $2\lambda$  is the spin splitting at the valence band top caused by the SOC and  $\hat{s}_z$  is the Pauli matrix for spin.



# $\vec{k} \cdot \vec{p}$ -method in action: Low-energy effective $H$

- Graphene: 2<sup>nd</sup> order perturbation theory**

Intrinsic and Rashba spin-orbit interactions in graphene sheet

→ PRB **74**, 165310 (2006); Mesoscopic interactions are

$$\hat{V} = \hat{H}_{SO} + \hat{H}_{EF} = \frac{1}{2(m_e c)^2} (\nabla \times \vec{p}) \cdot \vec{S} + eE \sum_i z_i$$

$i$  is the lattice site index

→ The 1<sup>st</sup> order perturbation in  $\vec{k} \cdot \vec{p}$ -method vanishes

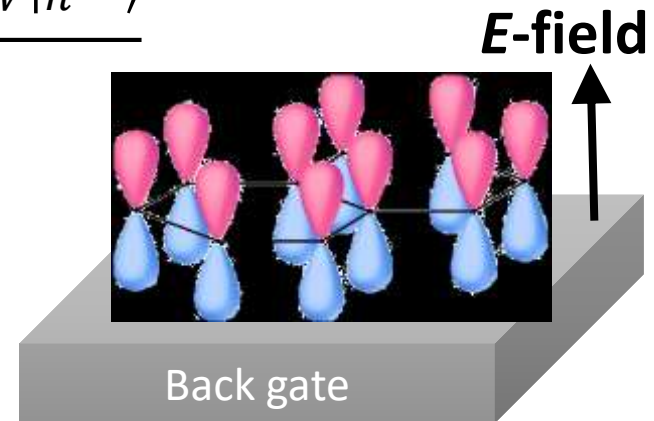
→ The 2<sup>nd</sup> degenerate perturbation

Leonard I. Schiff, *Quantum Mechanics*, McGraw-Hill, New York, (1968)

$$V_{m,n}^{(2)} = \sum_{l \notin D} \frac{\langle m^{(0)} | V | l^{(0)} \rangle \langle l^{(0)} | V | n^{(0)} \rangle}{E_E - E_l^{(0)}}$$

→ Low-energy sector

$$= \{ |K, p_z A, \uparrow\rangle, |K, p_z A, \downarrow\rangle, |K', p_z A, \uparrow\rangle, |K', p_z A, \downarrow\rangle, \\ |K, p_z B, \uparrow\rangle, |K, p_z B, \downarrow\rangle, |K', p_z B, \uparrow\rangle, |K', p_z B, \downarrow\rangle \}$$



→ Applicable to 2D TMD:  $p_z A \mapsto \phi_c$  &  $K, p_z B \mapsto \phi_v^+$  &  $K', p_z B \mapsto \phi_v^-$

# $\vec{k} \cdot \vec{p}$ -method in action: Low-energy effective $H$

- **Graphene: 2<sup>nd</sup> order perturbation theory**

Intrinsic and Rashba spin-orbit interactions in graphene sheet

→ PRB **74**, 165310 (2006); Mesoscopic interactions are

$$\hat{V} = \hat{H}_{SO} + \hat{H}_{EF} = \frac{1}{2(m_e c)^2} (\nabla \times \vec{p}) \cdot \vec{S} + eE \sum_i z_i$$

$i$  is the lattice site index

→ **Mesoscopic Spin-orbit & Rashba interaction**

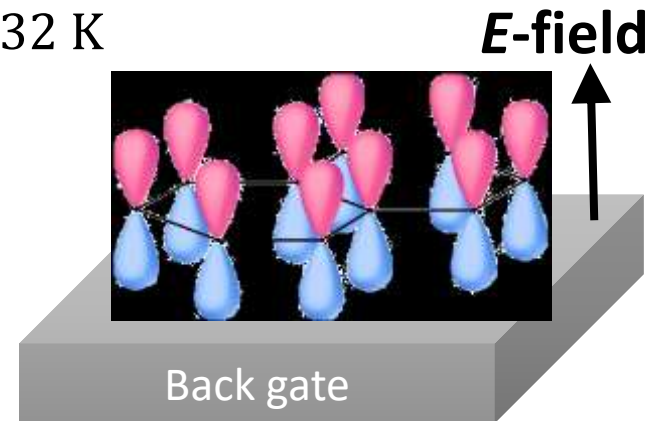
$$V_{\text{eff}} = -\lambda_{SO} + \lambda_{SO} \sigma_z \tau_z s_z + \lambda_R (\sigma_x \tau_z s_y - \sigma_z s_x)$$

→ Dirac point at K(K')-valley opens a gap  $E_g = 2(\lambda_{SO} - \lambda_R)$

$$\rightarrow 2\lambda_{SO} = \frac{|s|}{9(sp\sigma)^2} \xi^2 \approx 0.00114 \text{ meV} \approx k_B \times 0.0132 \text{ K}$$

$$\rightarrow \lambda_R = \frac{eEz_0}{3(sp\sigma)} \xi \propto E$$

Mesoscopic interactions depend on the shape of wavefunctions at low-energy



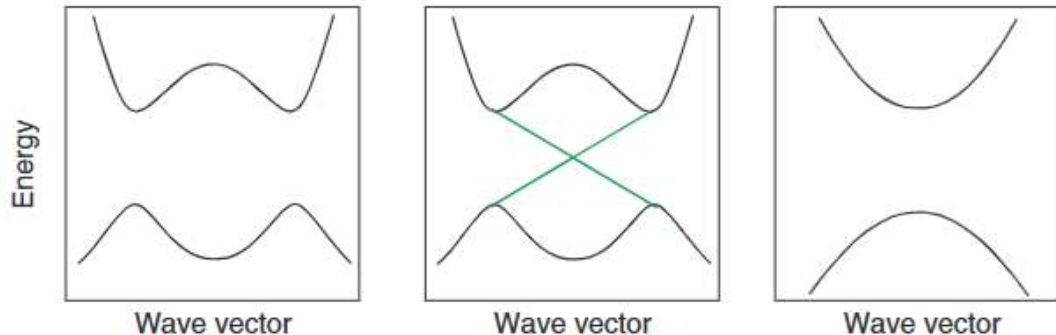
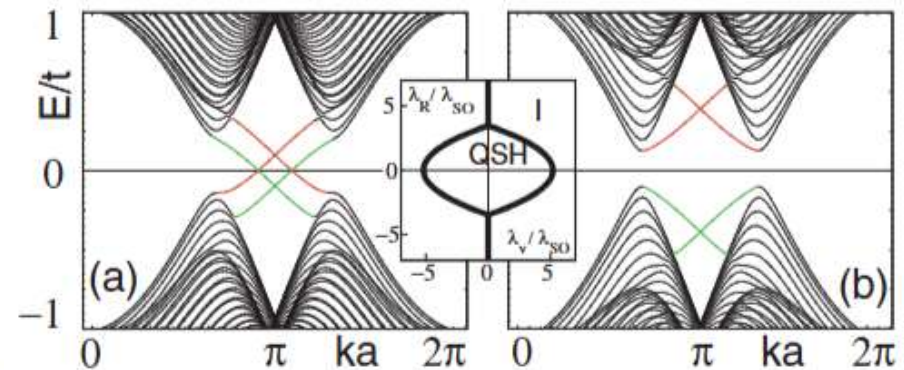
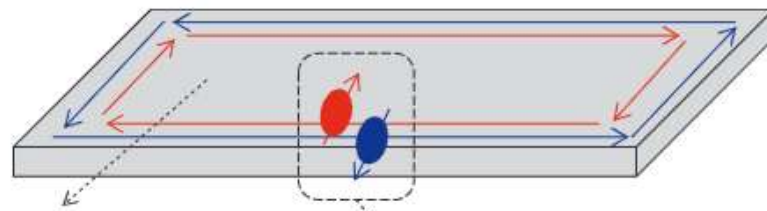
# $\vec{k} \cdot \vec{p}$ -method in action: Low-energy effective $H$

- **Graphene as 2D Topological Insulator (TI)**

→ PRL **95**, 226801 (2005); Quantum Spin Hall Effect in Graphene

→ PRL **95**, 146802 (2005); Z2 Topological Order and the Quantum Spin Hall Effect

→ Basically, 2D TIs realize  
the effective  $H$  of graphene



$$\lambda_{SO} \approx k_B \times 0.0066 \text{ K}$$

$$\lambda_R \approx k_B \times 0.129 \text{ K}$$

$$\lambda_R/\lambda_{SO} \approx 20$$

# What is Mesoscopic Quantum Transport

- **Low-energy effective Hamiltonian:  $\vec{k} \cdot \vec{p}$ -method**

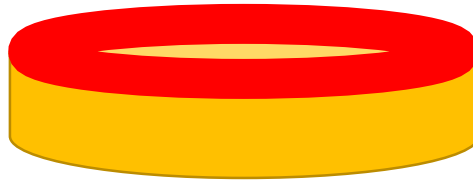
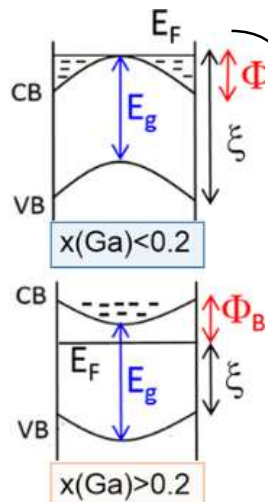
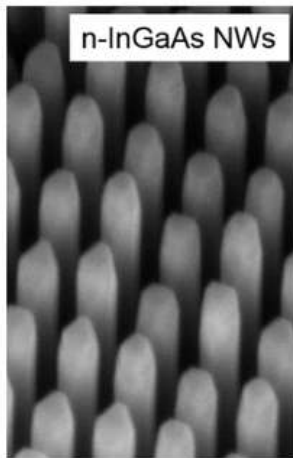
→ 1D InAs Nanowire?



$p_x$  →

→ Nano Letters 16, 5135 (2016)

Direct Measurements of Fermi Level Pinning at the Surface of Intrinsically n-Type InGaAs Nanowires



Select low-energy sector with  $|p_x = 0, \uparrow\rangle$  &  $|p_x = 0, \downarrow\rangle$

$$H_{\text{eff}}(p_x) = \begin{pmatrix} \langle 0, \uparrow | \hat{H}(p_x) | 0, \uparrow \rangle & \langle 0, \uparrow | \hat{H}(p_x) | 0, \downarrow \rangle \\ \langle 0, \downarrow | \hat{H}(p_x) | 0, \uparrow \rangle & \langle 0, \downarrow | \hat{H}(p_x) | 0, \downarrow \rangle \end{pmatrix}$$

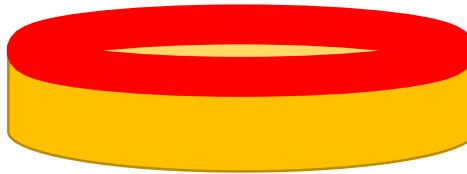
Strength of Mesoscopic interaction will vary



# What is Mesoscopic Quantum Transport

- **Low-energy effective Hamiltonian:  $\vec{k} \cdot \vec{p}$ -method**

→ 1D InAs Nanowire?



Select low-energy sector with  
 $|p_x = 0, \uparrow\rangle$  &  $|p_x = 0, \downarrow\rangle$

$$H_{\text{eff}}(p_x) = \begin{pmatrix} \langle 0, \uparrow | \hat{H}(p_x) | 0, \uparrow \rangle & \langle 0, \uparrow | \hat{H}(p_x) | 0, \downarrow \rangle \\ \langle 0, \downarrow | \hat{H}(p_x) | 0, \uparrow \rangle & \langle 0, \downarrow | \hat{H}(p_x) | 0, \downarrow \rangle \end{pmatrix}$$

- **Mesoscopic Zeeman Interaction  $\neq$  Bare Zeeman interaction**

→ Very high Landé g-factor,  $g \approx 14$  ( $g \approx 2$  for bare electrons)

$$H_Z = -\vec{\mu} \cdot \vec{B} = g\mu_B \vec{S} \cdot \vec{B}$$

→ Tunable Landé g-factor: PRB **72**, 201307(R) (2005)

→ Tunable Spin-orbit interaction: Nanoscale Adv. **4**, 2642 (2022)

# Overview

- **Recap. of the last lecture: Mesoscopic Quantum Transport (MQT)**  
→ It has been exactly 1 year!
- **MQT and low-energy theory in condensed matter systems**  
→ Low-energy effective theory by  $\vec{k} \cdot \vec{p}$ -method
- **$\vec{k} \cdot \vec{p}$ -method & Mesoscopic Interactions**  
→ Mesoscopic Spin-orbit, Rashba, Zeeman interactions
- **MQT in action**  
→  $\frac{dI}{dV}$  of topological systems calculating S-matrix
- **What left beyond today's lecture**

**Mesoscopic Quantum Transport in 2 hours!**



# MQT in action: $\frac{dI}{dV}$ of topological system from S-matrix

- Reproducing journal papers: Quantum Transport in TSC

→ PRL **102**, 216403 (2009), PRL **102**, 216404 (2009), and PRL **103**, 237001 (2009)

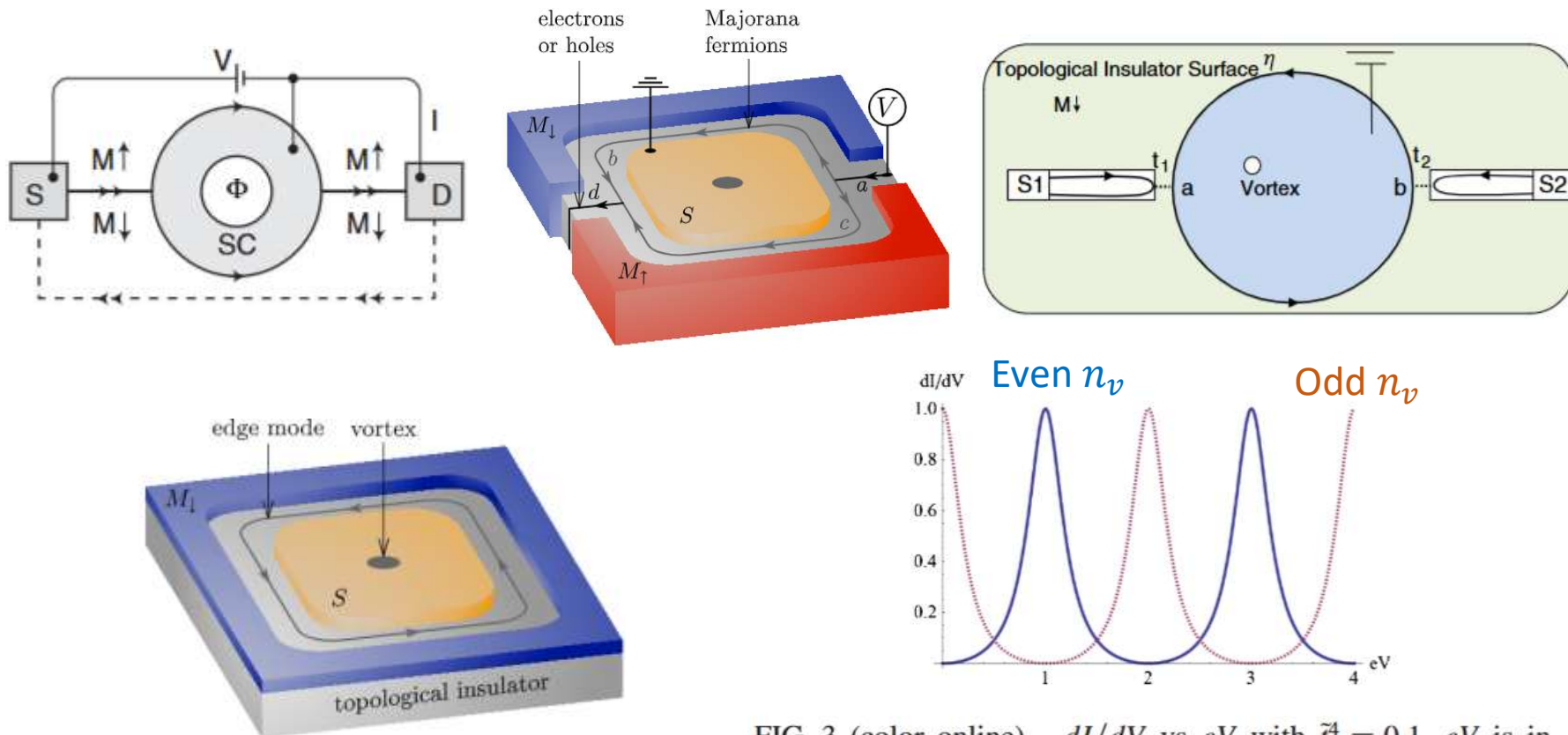
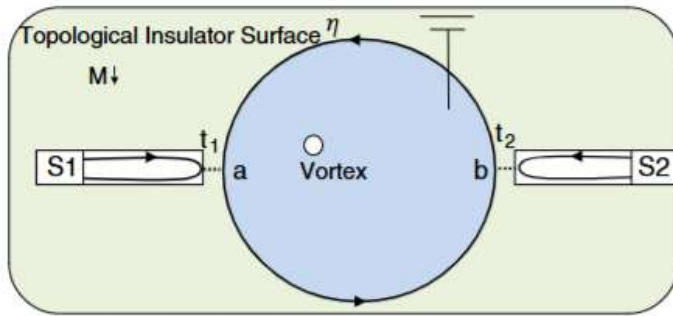


FIG. 3 (color online).  $dI/dV$  vs  $eV$  with  $\tilde{t}_1^4 = 0.1$ .  $eV$  is in units of  $\pi\hbar v_m/L$  and  $dI/dV$  is in units of  $\frac{2e^2}{h}$ . Solid (dashed) line represents the case with even (odd) number of vortices in the superconductor.

# MQT in action: $\frac{dI}{dV}$ of topological system from S-matrix

## • Quantum Transport in TSC

→ Majorana zero modes (MZM) always come in pair



Conductance quantum, as MZM = equal superposition of electron & hole

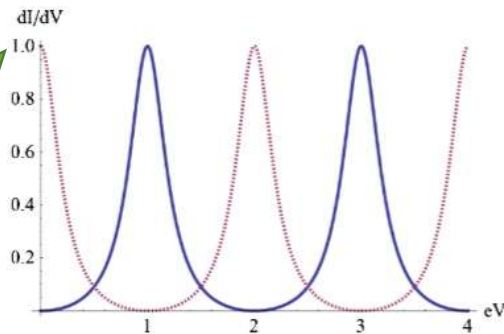
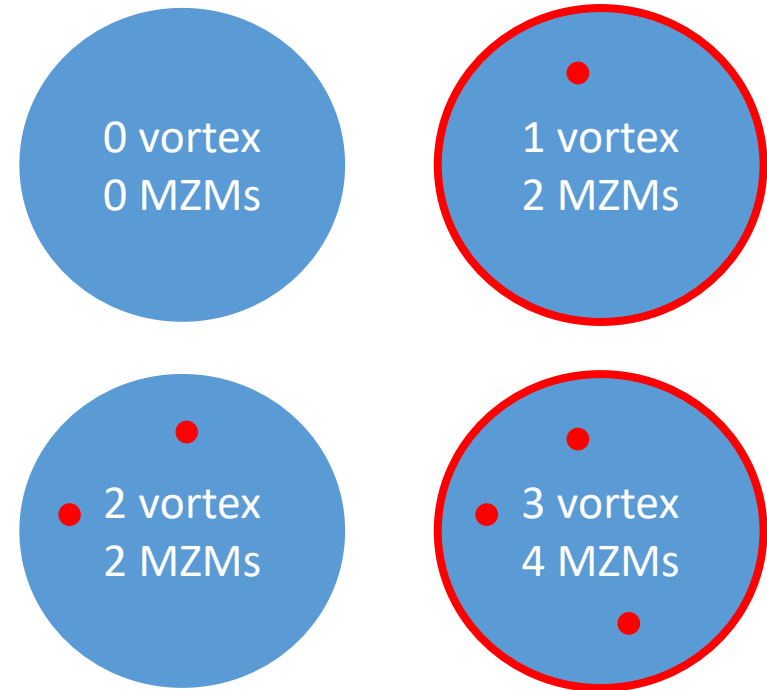


FIG. 3 (color online).  $dI/dV$  vs  $eV$  with  $\tilde{r}_1^4 = 0.1$ .  $eV$  is in units of  $\pi\hbar v_m/L$  and  $dI/dV$  is in units of  $\frac{2e^2}{h}$ . Solid (dashed) line represents the case with even (odd) number of vortices in the superconductor.



**Quantization condition along BC**

$$kL + \pi + n_v\pi = 2m\pi,$$

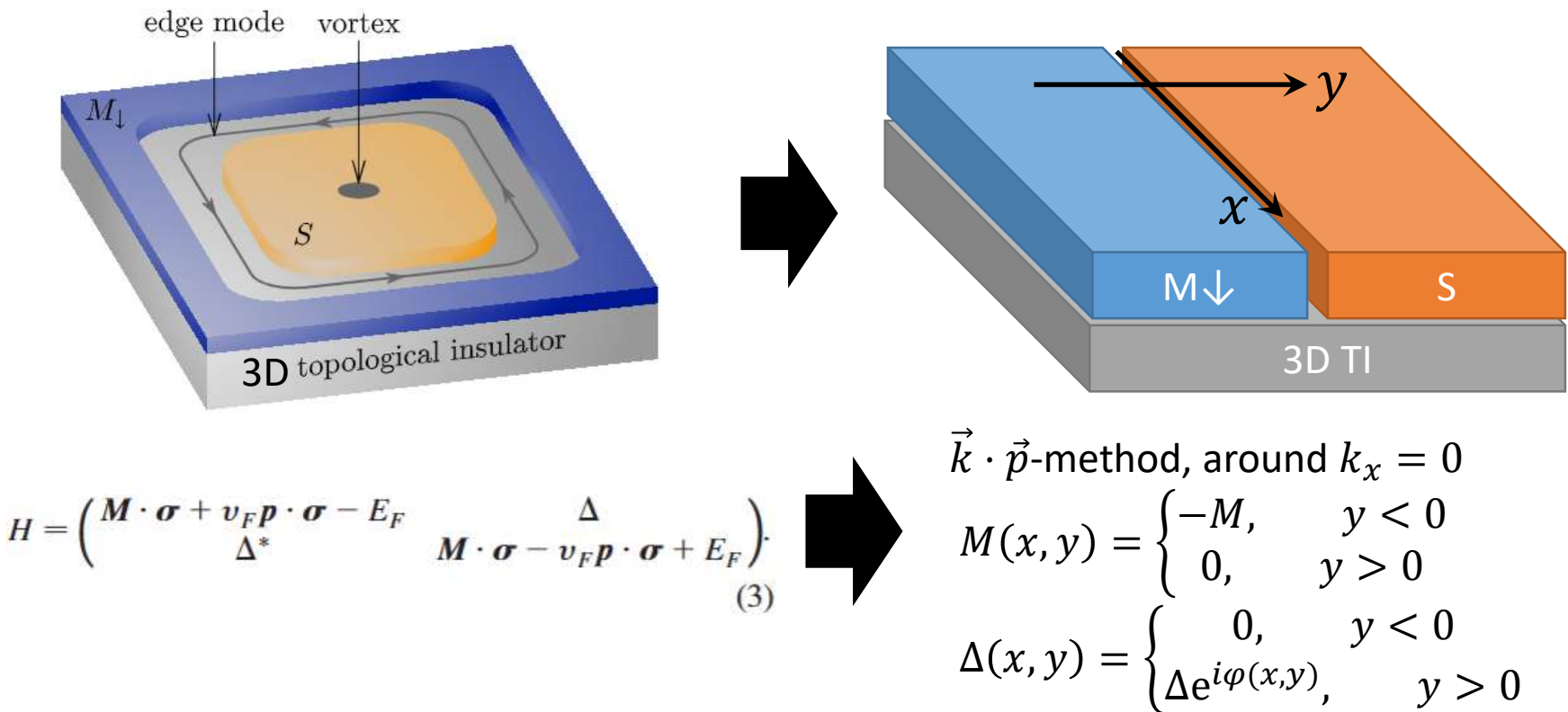
where  $n_v$  is # of vortices.

Electrically Detected Interferometry of Majorana Fermions in a Topological Insulator

A. R. Akhmerov, Johan Nilsson, and C. W. J. Beenakker

*Instituut-Lorentz, Universiteit Leiden, P.O. Box 9506, 2300 RA Leiden, The Netherlands*

(Received 16 March 2009; published 28 May 2009)



# MQT in action: $\frac{dI}{dV}$ of topological system from S-matrix

## • Low-energy Hamiltonian

$$H(p_x = 0)$$

$$= \begin{pmatrix} -M\sigma_z - i\hbar v_F \partial_y \sigma_y & 0 \\ 0 & -M\sigma_z + i\hbar v_F \partial_y \sigma_y \end{pmatrix} \Theta(-y) + \begin{pmatrix} -i\hbar v_F \partial_y \sigma_y & \Delta e^{i\varphi} \\ \Delta e^{-i\varphi} & +i\hbar v_F \partial_y \sigma_y \end{pmatrix} \Theta(y)$$

$$= \begin{pmatrix} -M & -\hbar v_F \partial_y & 0 & 0 \\ \hbar v_F \partial_y & M & 0 & 0 \\ 0 & 0 & -M & \hbar v_F \partial_y \\ 0 & 0 & -\hbar v_F \partial_y & M \end{pmatrix} \Theta(-y) + \begin{pmatrix} 0 & -\hbar v_F \partial_y & \Delta e^{i\varphi} & 0 \\ \hbar v_F \partial_y & 0 & 0 & \Delta e^{i\varphi} \\ \Delta e^{-i\varphi} & 0 & 0 & -\hbar v_F \partial_y \\ 0 & \Delta e^{-i\varphi} & \hbar v_F \partial_y & 0 \end{pmatrix} \Theta(y)$$

## Zero-energy solutions

Region:  $y < 0$

$$\psi(y) \propto e^{\frac{M}{\hbar v_F} y} \left[ A \begin{pmatrix} 1 \\ -1 \\ 0 \\ 0 \end{pmatrix} + B \begin{pmatrix} 0 \\ 0 \\ 1 \\ 1 \end{pmatrix} \right]$$

Region:  $y > 0$

$$\psi(y) \propto e^{-\frac{\Delta}{\hbar v_F} y} \left[ C \begin{pmatrix} e^{\frac{i\varphi}{2}} \\ 0 \\ 0 \\ e^{-\frac{i\varphi}{2}} \end{pmatrix} + D \begin{pmatrix} 0 \\ e^{\frac{i\varphi}{2}} \\ -e^{-\frac{i\varphi}{2}} \\ 0 \end{pmatrix} \right]$$

# MQT in action: $\frac{dI}{dV}$ of topological system from S-matrix

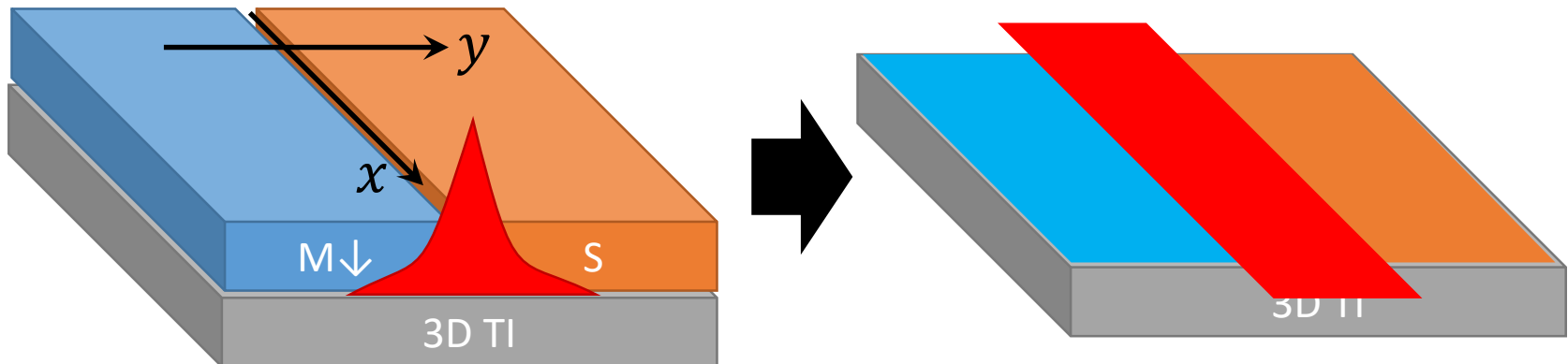
- Wave function matching at  $y=0$

$$A \begin{pmatrix} 1 \\ -1 \\ 0 \\ 0 \end{pmatrix} + B \begin{pmatrix} 0 \\ 0 \\ 1 \\ 1 \end{pmatrix} = C \begin{pmatrix} e^{\frac{i\varphi}{2}} \\ 0 \\ 0 \\ e^{-\frac{i\varphi}{2}} \end{pmatrix} + D \begin{pmatrix} 0 \\ e^{\frac{i\varphi}{2}} \\ -e^{-\frac{i\varphi}{2}} \\ 0 \end{pmatrix} \Leftrightarrow \begin{pmatrix} 0 \\ 0 \\ 0 \\ 0 \end{pmatrix} = \tilde{Q} \begin{pmatrix} A \\ B \\ C \\ D \end{pmatrix}$$

$$\tilde{Q} = \begin{pmatrix} 1 & 0 & -e^{\frac{i\varphi}{2}} & 0 \\ -1 & 0 & 0 & -e^{\frac{i\varphi}{2}} \\ 0 & 1 & 0 & e^{-\frac{i\varphi}{2}} \\ 0 & 1 & -e^{-\frac{i\varphi}{2}} & 0 \end{pmatrix}$$

$\det \tilde{Q} = 0 \Leftrightarrow$  There exists the topological zero-energy state.

$$A = -e^{\frac{i\varphi}{2}}, B = -e^{-\frac{i\varphi}{2}}, C = -1, D = 1$$





# MQT in action: $\frac{dI}{dV}$ of topological system from S-matrix

- Wave function matching at  $y=0$

$$A \begin{pmatrix} 1 \\ -1 \\ 0 \\ 0 \end{pmatrix} + B \begin{pmatrix} 0 \\ 0 \\ 1 \\ 1 \end{pmatrix} = C \begin{pmatrix} e^{\frac{i\varphi}{2}} \\ 0 \\ 0 \\ e^{-\frac{i\varphi}{2}} \end{pmatrix} + D \begin{pmatrix} 0 \\ e^{\frac{i\varphi}{2}} \\ -e^{-\frac{i\varphi}{2}} \\ 0 \end{pmatrix} \Leftrightarrow \begin{pmatrix} 0 \\ 0 \\ 0 \\ 0 \end{pmatrix} = \tilde{Q} \begin{pmatrix} A \\ B \\ C \\ D \end{pmatrix}$$

$$\tilde{Q} = \begin{pmatrix} 1 & 0 & -e^{\frac{i\varphi}{2}} & 0 \\ -1 & 0 & 0 & -e^{\frac{i\varphi}{2}} \\ 0 & 1 & 0 & e^{-\frac{i\varphi}{2}} \\ 0 & 1 & -e^{-\frac{i\varphi}{2}} & 0 \end{pmatrix}$$

$\det \tilde{Q} = 0 \Leftrightarrow$  There exists the topological zero-energy state.

$$A = e^{\frac{i\varphi}{2}}, B = e^{-\frac{i\varphi}{2}}, C = 1, D = -1$$

If  $M = \Delta$ , analytical expression is simple

$$\psi(y) \propto e^{-\frac{\Delta}{\hbar v_F} |y|} \begin{pmatrix} e^{\frac{i\varphi}{2}} \\ -e^{\frac{i\varphi}{2}} \\ e^{-\frac{i\varphi}{2}} \\ e^{-\frac{i\varphi}{2}} \end{pmatrix}$$

Particle-hole symmetry is expressed by the anticommutation  $H\Xi = -\Xi H$  of the Hamiltonian with the operator

$$\Xi = \begin{pmatrix} 0 & i\sigma_y \mathcal{C} \\ -i\sigma_y \mathcal{C} & 0 \end{pmatrix}, \quad (4)$$

Try checking  $\Xi \psi(y) = \psi(y)$ : Majorana mode



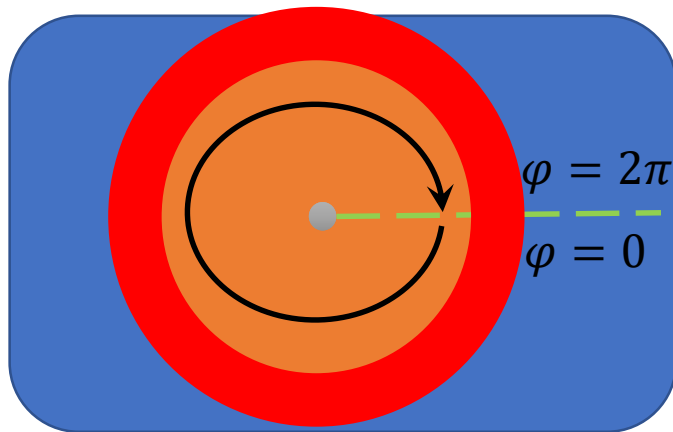
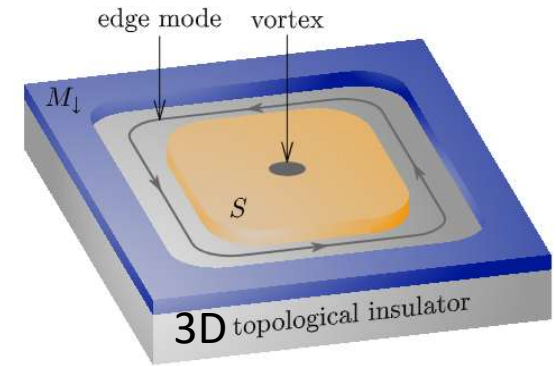
# MQT in action: $\frac{dI}{dV}$ of topological system from S-matrix

- **Low-energy Hamiltonian: chiral Majorana mode**

$$H_{\text{eff}}(p_x) = \int_{-\infty}^{\infty} \psi^\dagger(y) H(p_x, -i\hbar\partial_y) \psi(y) dy \propto -\hbar v_F p_x$$

- **Recall basis of the chiral Majorana mode**

$$\psi(y) \propto e^{-\frac{\Delta}{\hbar v_F} |y|} \begin{pmatrix} e^{\frac{i\varphi}{2}} \\ -e^{\frac{i\varphi}{2}} \\ e^{-\frac{i\varphi}{2}} \\ e^{-\frac{i\varphi}{2}} \end{pmatrix}, \text{ where } \varphi = \varphi(\vec{r}) \text{ and } \vec{r} \in S$$



For  $\varphi \mapsto \varphi + 2\pi$ ,  $\psi(y)$  accumulates  $\pi$ -phase

$$\text{For } \varphi \mapsto \varphi + 2\pi, \begin{pmatrix} e^{\frac{i\varphi}{2}} \\ -e^{\frac{i\varphi}{2}} \\ e^{-\frac{i\varphi}{2}} \\ e^{-\frac{i\varphi}{2}} \end{pmatrix} \mapsto - \begin{pmatrix} e^{\frac{i\varphi}{2}} \\ -e^{\frac{i\varphi}{2}} \\ e^{-\frac{i\varphi}{2}} \\ e^{-\frac{i\varphi}{2}} \end{pmatrix}$$

# MQT in action: $\frac{dI}{dV}$ of topological system from S-matrix

- **Low-energy Hamiltonian: chiral Majorana mode**

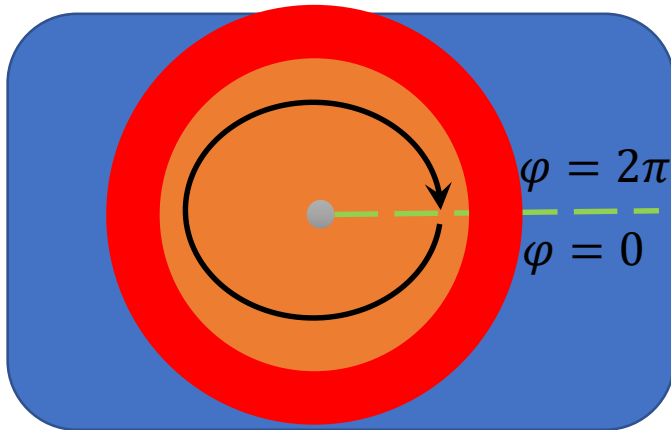
$$H_{\text{eff}}(p_x) = \int_{-\infty}^{\infty} \psi^\dagger(y) H(p_x, -i\hbar\partial_y) \psi(y) dy \propto -\hbar v_m p_x$$

- **Recall basis of the chiral Majorana mode**

$$\psi(y) \propto e^{-\frac{\Delta}{\hbar v_F} |y|} \begin{pmatrix} e^{\frac{i\varphi}{2}} \\ -e^{\frac{i\varphi}{2}} \\ e^{-\frac{i\varphi}{2}} \\ e^{-\frac{i\varphi}{2}} \end{pmatrix}, \text{ where } \varphi = \varphi(\vec{r}) \text{ and } \vec{r} \in S$$

**Mesoscopic Interaction  
may renormalize  $v_F$**

$$v_m = v_F \frac{\sqrt{1 - \left(\frac{E_F}{M}\right)^2}}{1 + \frac{E_F}{\Delta}}$$



For  $\varphi \mapsto \varphi + 2\pi$ ,  $\psi(y)$  accumulates  $\pi$ -phase

$$\text{For } \varphi \mapsto \varphi + 2\pi, \begin{pmatrix} e^{\frac{i\varphi}{2}} \\ -e^{\frac{i\varphi}{2}} \\ e^{-\frac{i\varphi}{2}} \\ e^{-\frac{i\varphi}{2}} \end{pmatrix} \mapsto - \begin{pmatrix} e^{\frac{i\varphi}{2}} \\ -e^{\frac{i\varphi}{2}} \\ e^{-\frac{i\varphi}{2}} \\ e^{-\frac{i\varphi}{2}} \end{pmatrix}$$

# MQT in action: $\frac{dI}{dV}$ of topological system from S-matrix

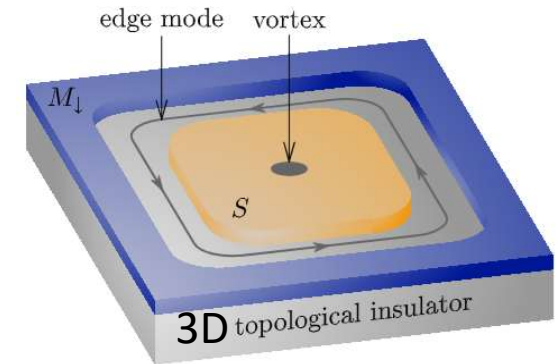
- **Low-energy Hamiltonian: chiral Majorana mode**

$$H_{\text{eff}}(p_x) = \int_{-\infty}^{\infty} \psi^\dagger(y) H(p_x, -i\hbar\partial_y) \psi(y) dy \propto -\hbar v_m p_x$$

- **The quantization condition:**

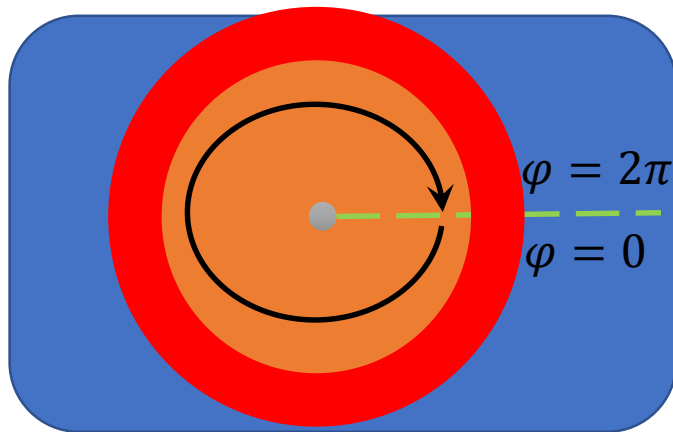
as  $\psi(y)$  accumulates  $\pi$ -phase For  $\varphi \mapsto \varphi + 2\pi$ ,

$$kL + \pi + n_v\pi = 2m\pi$$



**Berry phase**

Below spinor rotates along boundary



$$\psi(y) \propto e^{-\frac{\Delta}{\hbar v_F}|y|} \begin{pmatrix} e^{\frac{i\varphi}{2}} \\ -e^{\frac{i\varphi}{2}} \\ e^{-\frac{i\varphi}{2}} \\ -e^{-\frac{i\varphi}{2}} \end{pmatrix}$$

# MQT in action: $\frac{dI}{dV}$ of topological system from S-matrix

- Low-energy Hamiltonian: chiral Majorana mode

$$H_{\text{eff}}(p_x) = \int_{-\infty}^{\infty} \psi^\dagger(y) H(p_x, -i\hbar\partial_y) \psi(y) dy \propto -\hbar v_m p_x$$

- The quantization condition:

$$kL + \pi + n_v\pi = 2m\pi$$

- Quantized Energies

$$E_n = \hbar v_m k_n$$

$$= (2n - 1 - n_v) \frac{\pi \hbar v_F}{L}$$

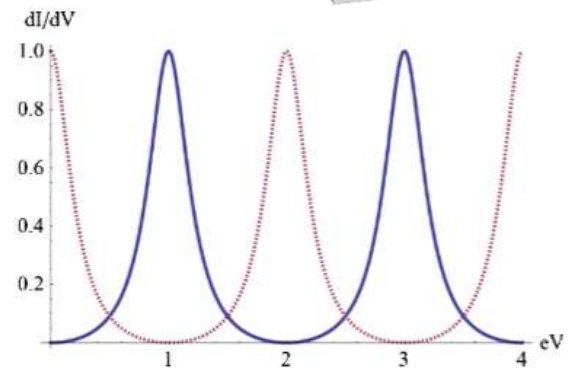
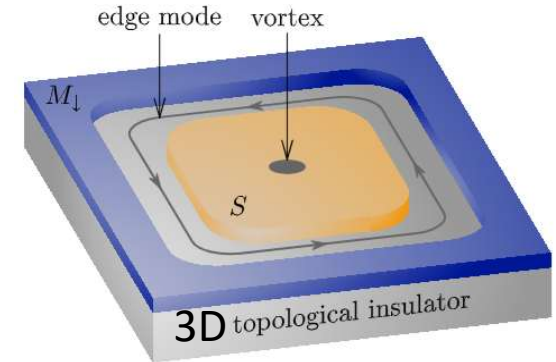


FIG. 3 (color online).  $dI/dV$  vs  $eV$  with  $\tilde{t}_1^4 = 0.1$ .  $eV$  is in units of  $\pi \hbar v_m / L$  and  $dI/dV$  is in units of  $\frac{2e^2}{h}$ . Solid (dashed) line represents the case with even (odd) number of vortices in the superconductor.

# MQT in action: $\frac{dI}{dV}$ of topological system from S-matrix

- **Low-energy Hamiltonian: chiral Majorana mode**

$$H_{\text{eff}}(p_x) = \int_{-\infty}^{\infty} \psi^\dagger(y) H(p_x, -i\hbar\partial_y) \psi(y) dy \propto -\hbar v_m p_x$$

- **The quantization condition:**

$$kL + \pi + n_v\pi = 2m\pi$$

- **Quantized Energies**

$$E_n = \hbar v_F k_n$$

$$= (2n - 1 - n_v) \frac{\pi \hbar v_F}{L}$$

Conductance quantum, as MZM = equal superposition of electron & hole

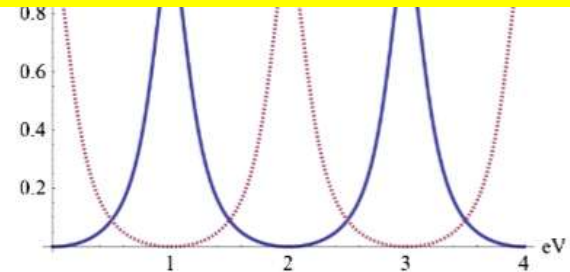
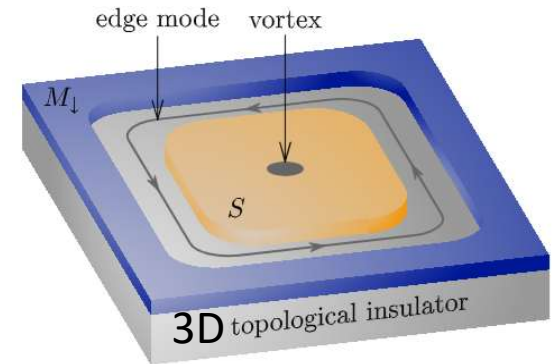


FIG. 3 (color online).  $dI/dV$  vs  $eV$  with  $\tilde{t}_1^4 = 0.1$ .  $eV$  is in units of  $\pi \hbar v_m / L$  and  $dI/dV$  is in units of  $\frac{2e^2}{h}$ . Solid (dashed) line represents the case with even (odd) number of vortices in the superconductor.

# MQT in action: $\frac{dI}{dV}$ of topological system from S-matrix

- **Try:** derive the low-energy Hamiltonian of below

using  $\vec{k} \cdot \vec{p}$ -method (it should be chiral electron & hole modes)

$$H(p_x = 0) = \begin{pmatrix} -M & -\hbar v_F \partial_y & 0 & 0 \\ \hbar v_F \partial_y & M & 0 & 0 \\ 0 & 0 & -M & \hbar v_F \partial_y \\ 0 & 0 & -\hbar v_F \partial_y & M \end{pmatrix} \Theta(-y) + \begin{pmatrix} M & -\hbar v_F \partial_y & 0 & 0 \\ \hbar v_F \partial_y & -M & 0 & 0 \\ 0 & 0 & M & -\hbar v_F \partial_y \\ 0 & 0 & \hbar v_F \partial_y & -M \end{pmatrix} \Theta(y)$$

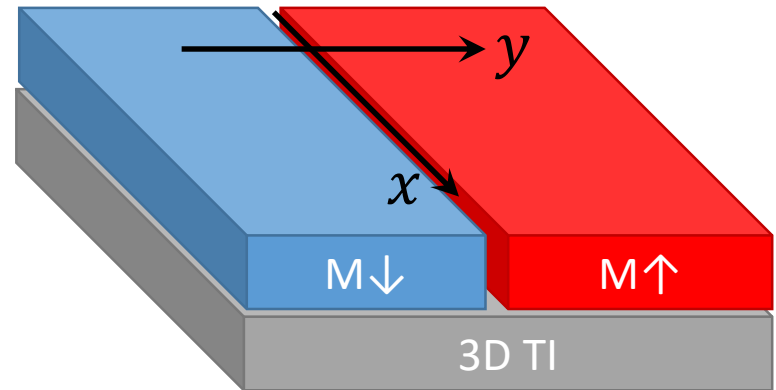
## Zero-energy solutions

Region:  $y < 0$

$$\psi(y) \propto e^{\frac{M}{\hbar v_F} y} \left[ A \begin{pmatrix} 1 \\ -1 \\ 0 \\ 0 \end{pmatrix} + B \begin{pmatrix} 0 \\ 0 \\ 1 \\ 1 \end{pmatrix} \right]$$

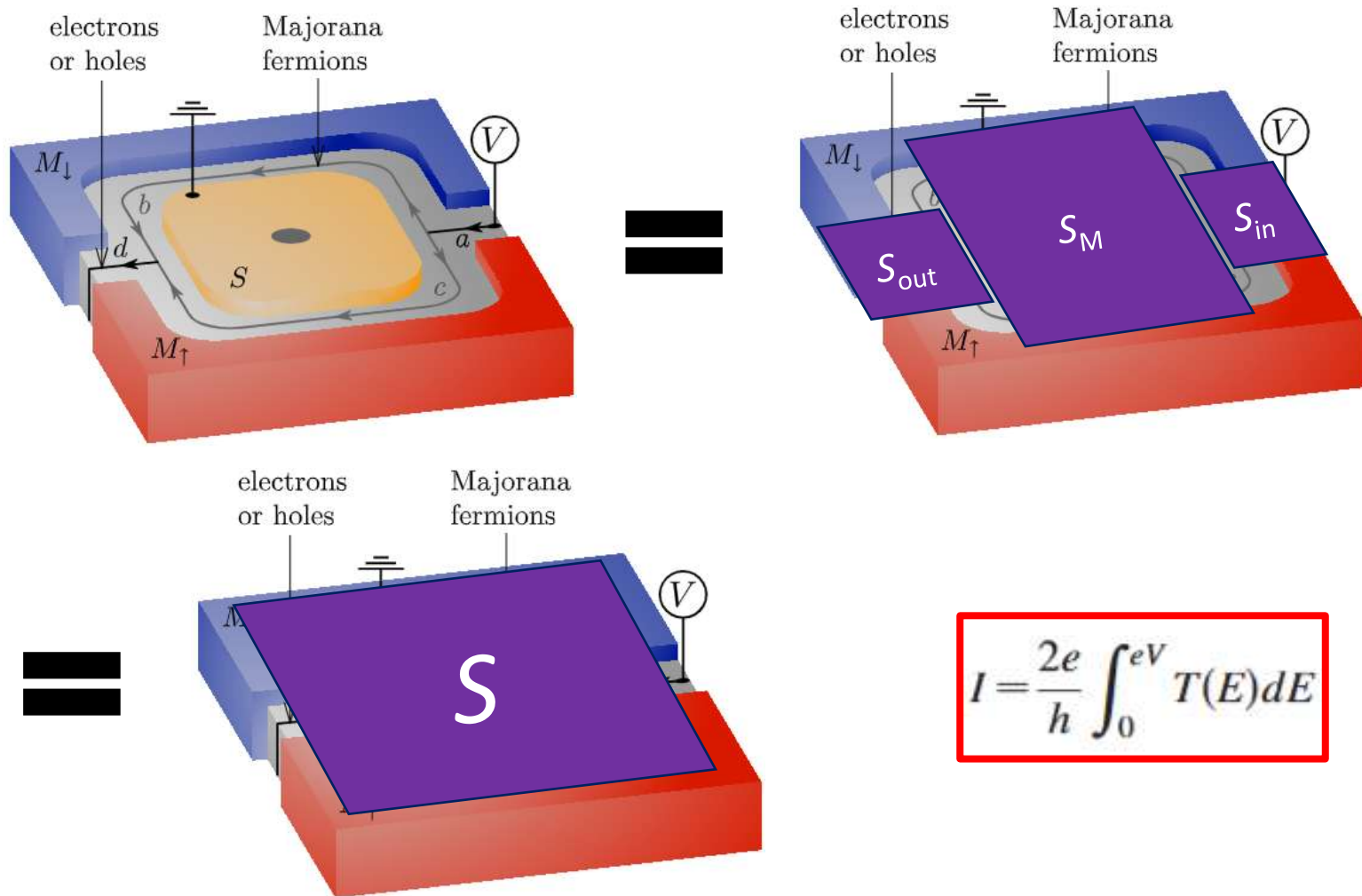
Region:  $y > 0$

$$\psi(y) \propto e^{-\frac{M}{\hbar v_F} y} \left[ C \begin{pmatrix} 1 \\ -1 \\ 0 \\ 0 \end{pmatrix} + D \begin{pmatrix} 0 \\ 0 \\ 1 \\ 1 \end{pmatrix} \right]$$



# MQT in action: $\frac{dI}{dV}$ of topological system from S-matrix

- Mesoscopic Quantum Transport in TSC using S-matrix



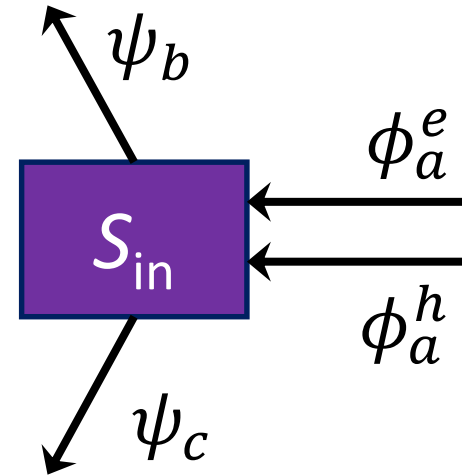
# MQT in action: $\frac{dI}{dV}$ of topological system from S-matrix

- Symmetry of  $S_{\text{in}}$ -matrix: particle-hole**

$$\begin{pmatrix} \psi_b \\ \psi_c \end{pmatrix} = S_{\text{in}} \begin{pmatrix} \phi_a^e \\ \phi_a^h \end{pmatrix}. \quad (5)$$

Particle-hole symmetry for the scattering matrix is expressed by

$$S_{\text{in}}(\varepsilon) = S_{\text{in}}^*(-\varepsilon) \begin{pmatrix} 0 & 1 \\ 1 & 0 \end{pmatrix}. \quad (6)$$



$\rightarrow |\Psi_{\text{in}}^E\rangle = \phi_a^e |\phi_a^e\rangle + \phi_a^h |\phi_a^h\rangle$  is an incoming state at energy  $E$ .

i.e.,  $\hat{H}|\Psi_N\rangle = E|\Psi_N\rangle$  with  $\hat{H}(\hat{\Xi}|\Psi_N\rangle) = -\hat{\Xi}\hat{H}\hat{\Xi}^{-1}(\hat{\Xi}|\Psi_N\rangle) = -E(\hat{\Xi}|\Psi_N\rangle)$

$\therefore \hat{\Xi}|\Psi_N\rangle$  is the energy eigenstate of  $-E$  and it's an incoming state.

$$\text{c.f., } \hat{\Xi}|\Psi_N\rangle = \hat{\Xi}(\phi_a^e |\phi_a^e\rangle + \phi_a^h |\phi_a^h\rangle) = (\phi_a^h)^* |\phi_a^e\rangle + (\phi_a^e)^* |\phi_a^h\rangle$$

$\therefore$  given incoming  $\begin{pmatrix} \phi_a^e \\ \phi_a^h \end{pmatrix}$  at  $E$ , incoming at  $-E$  is known  $\begin{pmatrix} (\phi_a^h)^* \\ (\phi_a^e)^* \end{pmatrix}$



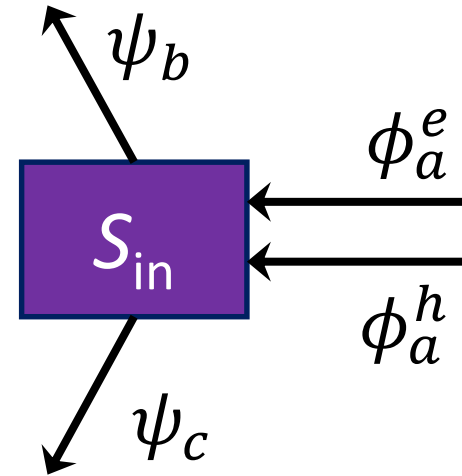
# MQT in action: $\frac{dI}{dV}$ of topological system from S-matrix

- Symmetry of  $S_{\text{in}}$ -matrix: particle-hole**

$$\begin{pmatrix} \psi_b \\ \psi_c \end{pmatrix} = S_{\text{in}} \begin{pmatrix} \phi_a^e \\ \phi_a^h \end{pmatrix}. \quad (5)$$

Particle-hole symmetry for the scattering matrix is expressed by

$$S_{\text{in}}(\varepsilon) = S_{\text{in}}^*(-\varepsilon) \begin{pmatrix} 0 & 1 \\ 1 & 0 \end{pmatrix}. \quad (6)$$



$\rightarrow |\Psi_{\text{in}}^E\rangle = \phi_a^e |\phi_a^e\rangle + \phi_a^h |\phi_a^h\rangle$  is an incoming state at energy  $E$ .

i.e.,  $\hat{H}|\Psi_{\text{in}}^E\rangle = E|\Psi_{\text{in}}^E\rangle$  with  $\hat{H}(\hat{\Xi}|\Psi_{\text{in}}^E\rangle) = -\hat{\Xi}\hat{H}\hat{\Xi}^{-1}(\hat{\Xi}|\Psi_{\text{in}}^E\rangle) = -E(\hat{\Xi}|\Psi_{\text{in}}^E\rangle)$

$\therefore \hat{\Xi}|\Psi_{\text{in}}^E\rangle$  is the energy eigenstate of  $-E$  and it's an incoming state.

c.f.,  $|\Psi_{\text{in}}^{-E}\rangle = \hat{\Xi}(\phi_a^e |\phi_a^e\rangle + \phi_a^h |\phi_a^h\rangle) = (\phi_a^h)^* |\phi_a^e\rangle + (\phi_a^e)^* |\phi_a^h\rangle$

$\therefore$  given incoming  $\begin{pmatrix} \phi_a^e \\ \phi_a^h \end{pmatrix}$  at  $E$ , incoming at  $-E$  is known  $\begin{pmatrix} (\phi_a^h)^* \\ (\phi_a^e)^* \end{pmatrix}$

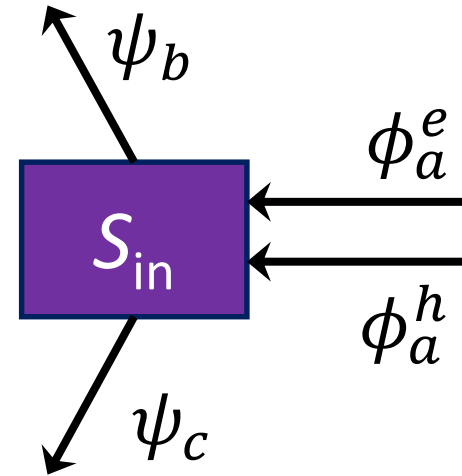
# MQT in action: $\frac{dI}{dV}$ of topological system from S-matrix

- Symmetry of  $S_{\text{in}}$ -matrix: particle-hole

$$\begin{pmatrix} \psi_b \\ \psi_c \end{pmatrix} = S_{\text{in}} \begin{pmatrix} \phi_a^e \\ \phi_a^h \end{pmatrix}. \quad (5)$$

Particle-hole symmetry for the scattering matrix is expressed by

$$S_{\text{in}}(\epsilon) = S_{\text{in}}^*(-\epsilon) \begin{pmatrix} 0 & 1 \\ 1 & 0 \end{pmatrix}. \quad (6)$$



$\rightarrow |\Psi_{b,c}^E\rangle = \psi_{b,c} |\psi_{b,c}\rangle$  is an outgoing state.

$\hat{E} |\Psi_{b,c}^E\rangle$  is the energy eigenstate of  $-E$  and it's an incoming state.

$$\text{c.f., } |\Psi_{b,c}^{-E}\rangle = \hat{E} (\psi_{b,c} |\psi_{b,c}\rangle) = \psi_{b,c}^* |\psi_{b,c}\rangle$$

$\therefore$  given outgoing  $\begin{pmatrix} \psi_b \\ \psi_c \end{pmatrix}$  at  $E$ , outgoing at  $-E$  is known  $\begin{pmatrix} \psi_b^* \\ \psi_c^* \end{pmatrix}$

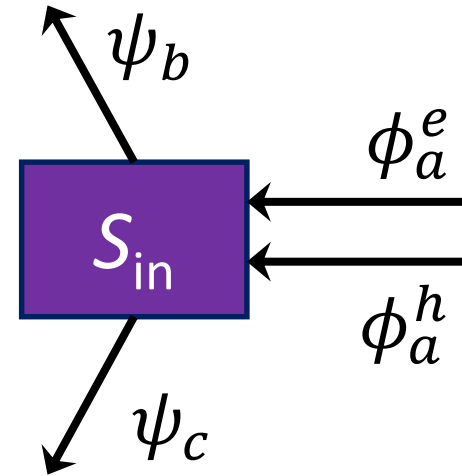
# MQT in action: $\frac{dI}{dV}$ of topological system from S-matrix

- Symmetry of  $S_{\text{in}}$ -matrix: particle-hole

$$\begin{pmatrix} \psi_b \\ \psi_c \end{pmatrix} = S_{\text{in}} \begin{pmatrix} \phi_a^e \\ \phi_a^h \end{pmatrix}. \quad (5)$$

Particle-hole symmetry for the scattering matrix is expressed by

$$S_{\text{in}}(\varepsilon) = S_{\text{in}}^*(-\varepsilon) \begin{pmatrix} 0 & 1 \\ 1 & 0 \end{pmatrix}. \quad (6)$$



→ given incoming  $\begin{pmatrix} \phi_a^e \\ \phi_a^h \end{pmatrix}$  at  $E$ , incoming at  $-E$  is known  $\begin{pmatrix} (\phi_a^h)^* \\ (\phi_a^e)^* \end{pmatrix}$

→ given outgoing  $\begin{pmatrix} \psi_b \\ \psi_c \end{pmatrix}$  at  $E$ , outgoing at  $-E$  is known  $\begin{pmatrix} \psi_b^* \\ \psi_c^* \end{pmatrix}$

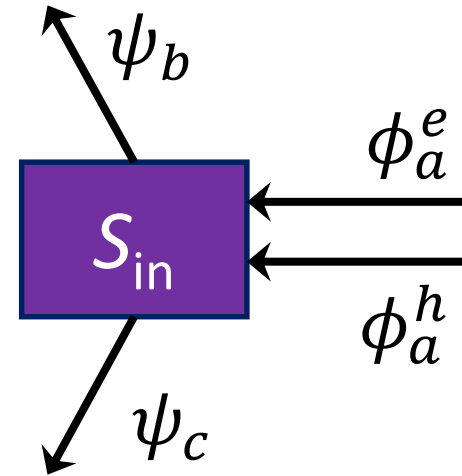
Hence,  $\begin{pmatrix} \psi_b^* \\ \psi_c^* \end{pmatrix} = S_{\text{in}}(-E) \begin{pmatrix} (\phi_a^h)^* \\ (\phi_a^e)^* \end{pmatrix} \Leftrightarrow \begin{pmatrix} \psi_b \\ \psi_c \end{pmatrix} = S_{\text{in}}^*(-E) \begin{pmatrix} 0 & 1 \\ 1 & 0 \end{pmatrix} \begin{pmatrix} \phi_a^e \\ \phi_a^h \end{pmatrix}$

# MQT in action: $\frac{dI}{dV}$ of topological system from S-matrix

- **Symmetry of  $S_{\text{in}}$ -matrix: particle-hole**

At small excitation energies  $|\varepsilon| \ll |M_z|, |\Delta|$  the  $\varepsilon$  dependence of  $S_{\text{in}}$  may be neglected. (The excitation energy is limited by the largest of voltage  $V$  and temperature  $T$ .) Then Eq. (6) together with unitarity ( $S_{\text{in}}^{-1} = S_{\text{in}}^\dagger$ ) fully determine the scattering matrix,

$$S_{\text{in}} = \frac{1}{\sqrt{2}} \begin{pmatrix} 1 & 1 \\ \pm i & \mp i \end{pmatrix} \begin{pmatrix} e^{i\alpha} & 0 \\ 0 & e^{-i\alpha} \end{pmatrix}, \quad (7)$$



→  $S_{\text{in}} = S_{\text{in}}^* \begin{pmatrix} 0 & 1 \\ 1 & 0 \end{pmatrix}$  and by using unitarity. The sign ambiguity &  $\alpha$  is undetermined but does not affect the conductance.

→ **Try!**

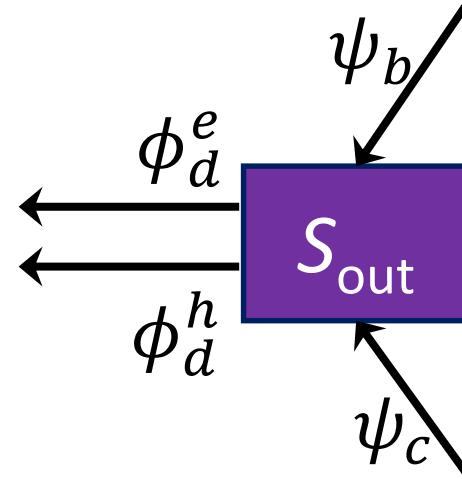
# MQT in action: $\frac{dI}{dV}$ of topological system from S-matrix

- Symmetry of  $S_{\text{out}}$ -matrix: time-reversal

The scattering matrix  $S_{\text{out}}$  for the conversion from Majorana modes to electron and hole modes can be obtained from  $S_{\text{in}}$  by time reversal,

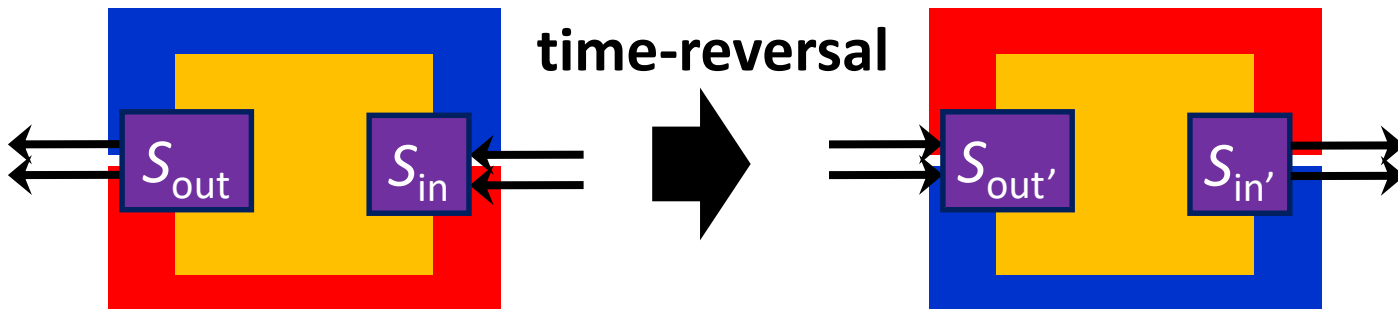
$$S_{\text{out}}(\mathbf{M}) = S_{\text{in}}^T(-\mathbf{M}) = \frac{1}{\sqrt{2}} \begin{pmatrix} e^{i\alpha'} & 0 \\ 0 & e^{-i\alpha'} \end{pmatrix} \begin{pmatrix} 1 & \pm i \\ 1 & \mp i \end{pmatrix}. \quad (8)$$

The phase shift  $\alpha'$  may be different from  $\alpha$ , because of the sign change of  $\mathbf{M}$  upon time reversal, but it will also drop out of the conductance.



→ Just use time-reversal symmetry!

→ **Try it!** (You've learned how to apply the time-reversal operator to a low-energy Hamiltonian & S-matrix)



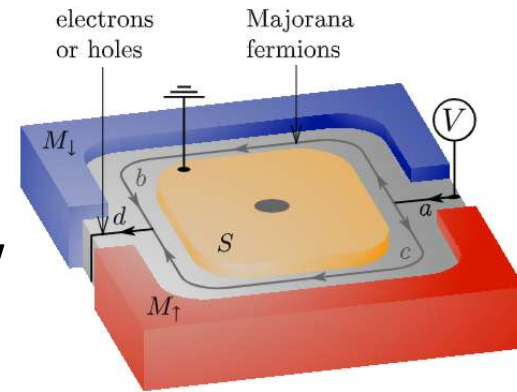
# MQT in action: $\frac{dI}{dV}$ of topological system from S-matrix

- $S_M$ -matrix

$$\begin{pmatrix} \psi_b \\ \psi_c \end{pmatrix}_{\text{out}} = \begin{pmatrix} e^{i\beta_b} & 0 \\ 0 & e^{i\beta_c} \end{pmatrix} \begin{pmatrix} \psi_b \\ \psi_c \end{pmatrix}_{\text{in}}$$

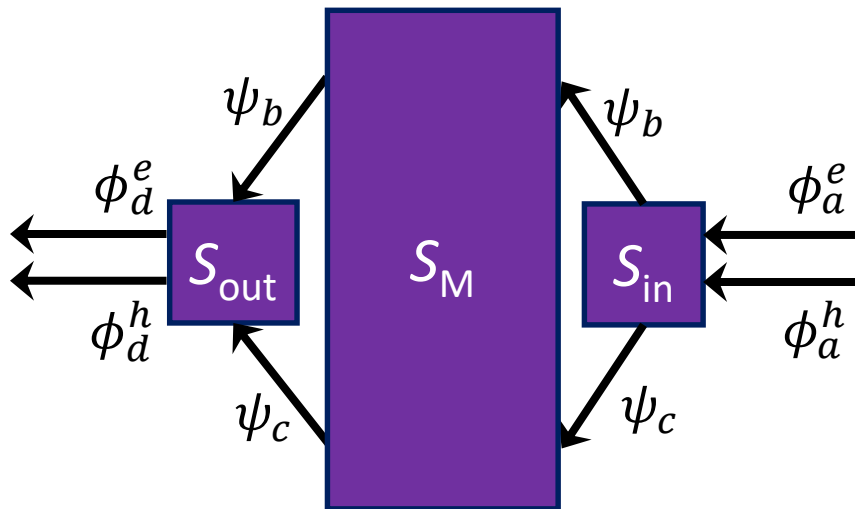
→ Just picking up phases with scattering. But we know

$$\beta_b - \beta_c = kL + \pi + n_v\pi = \frac{EL}{\hbar v_F} + \pi + n_v\pi$$



- S-matrix

$$S = \frac{1}{2} \begin{pmatrix} e^{i(\alpha+\alpha')}(e^{i\beta_b} - e^{i\beta_c}) & e^{-i(\alpha-\alpha')}(e^{i\beta_b} + e^{i\beta_c}) \\ e^{i(\alpha-\alpha')}(e^{i\beta_b} + e^{i\beta_c}) & e^{-i(\alpha+\alpha')}(e^{i\beta_b} - e^{i\beta_c}) \end{pmatrix}$$



The full scattering matrix  $S$  of the Mach-Zehnder interferometer in [Fig. 1](#) is given by the matrix product

$$S \equiv \begin{pmatrix} S_{ee} & S_{eh} \\ S_{he} & S_{hh} \end{pmatrix} = S_{\text{out}} \begin{pmatrix} e^{i\beta_b} & 0 \\ 0 & e^{i\beta_c} \end{pmatrix} S_{\text{in}}, \quad (9)$$

where  $\beta_b$  and  $\beta_c$  are the phase shifts accumulated by the Majorana modes along edge  $b$  and  $c$ , respectively. The relative phase

$$\beta_b - \beta_c = \varepsilon \delta L / \hbar v_m + \pi + n_v \pi \quad (10)$$

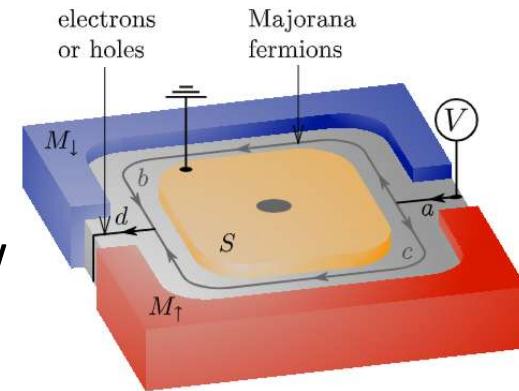
# MQT in action: $\frac{dI}{dV}$ of topological system from S-matrix

- **$S_M$ -matrix**

$$\begin{pmatrix} \psi_b \\ \psi_c \end{pmatrix}_{\text{out}} = \begin{pmatrix} e^{i\beta_b} & 0 \\ 0 & e^{i\beta_c} \end{pmatrix} \begin{pmatrix} \psi_b \\ \psi_c \end{pmatrix}_{\text{in}}$$

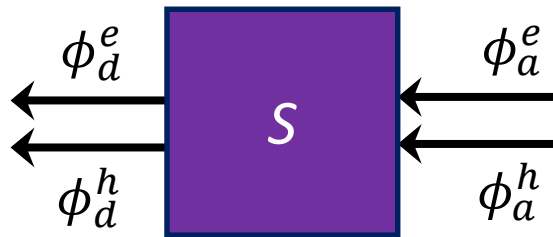
→ Just picking up phases with scattering. But we know

$$\beta_b - \beta_c = kL + \pi + n_v\pi = \frac{EL}{\hbar v_F} + \pi + n_v\pi$$



- **S-matrix**

$$S = \frac{1}{2} \begin{pmatrix} e^{i(\alpha+\alpha')}(e^{i\beta_b} - e^{i\beta_c}) & e^{-i(\alpha-\alpha')}(e^{i\beta_b} + e^{i\beta_c}) \\ e^{i(\alpha-\alpha')}(e^{i\beta_b} + e^{i\beta_c}) & e^{-i(\alpha+\alpha')}(e^{i\beta_b} - e^{i\beta_c}) \end{pmatrix}$$



$$\begin{pmatrix} \phi_d^e \\ \phi_d^h \end{pmatrix} = S \begin{pmatrix} \phi_a^e \\ \phi_a^h \end{pmatrix}, S = \begin{pmatrix} S_{ee} & S_{eh} \\ S_{he} & S_{hh} \end{pmatrix}$$

The full scattering matrix  $S$  of the Mach-Zehnder interferometer in [Fig. 1](#) is given by the matrix product

$$S \equiv \begin{pmatrix} S_{ee} & S_{eh} \\ S_{he} & S_{hh} \end{pmatrix} = S_{\text{out}} \begin{pmatrix} e^{i\beta_b} & 0 \\ 0 & e^{i\beta_c} \end{pmatrix} S_{\text{in}}, \quad (9)$$

where  $\beta_b$  and  $\beta_c$  are the phase shifts accumulated by the Majorana modes along edge  $b$  and  $c$ , respectively. The relative phase

$$\beta_b - \beta_c = \varepsilon \delta L / \hbar v_m + \pi + n_v \pi \quad (10)$$



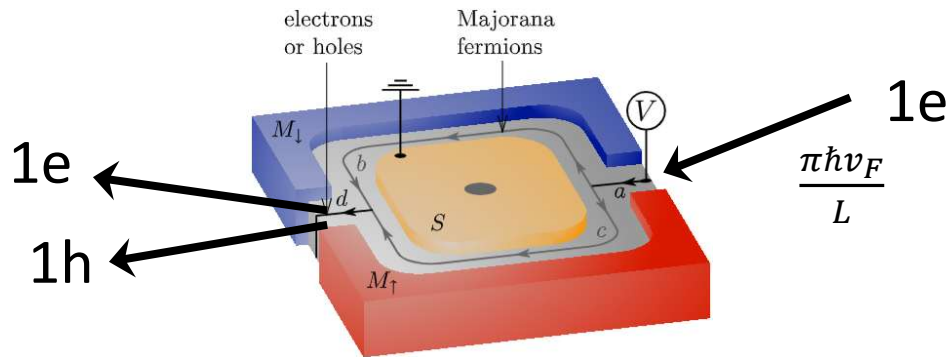
# MQT in action: $\frac{dI}{dV}$ of topological system from S-matrix

- Quantum Transport using Landauer-Büttiker

Negligible energy dependence of  $T(E)$

$$I = I(V) = \frac{e}{h} \int_{\mu_R}^{\mu_L} T(E) dE = \frac{e^2}{h} TV$$

→ Charge transmission into Superconductor



$$T = 1 - |S_{ee}|^2 + |S_{he}|^2 = 1 + |S_{he}|^2 - 1 + |S_{he}|^2 = 2|S_{he}|^2$$

from unitarity,  $|S_{ee}|^2 + |S_{he}|^2 = 1$

$$G(0) = \frac{2e^2}{h} \sin^2 \left( \frac{n_v \pi}{2} \right)$$

**Finally,**  $\frac{dI}{dV} = \frac{2e^2}{h} |S_{he}|^2 = \frac{2e^2}{h} \sin^2 \left( \frac{n_v \pi}{2} + \frac{eVL}{2\hbar v_F} \right)$

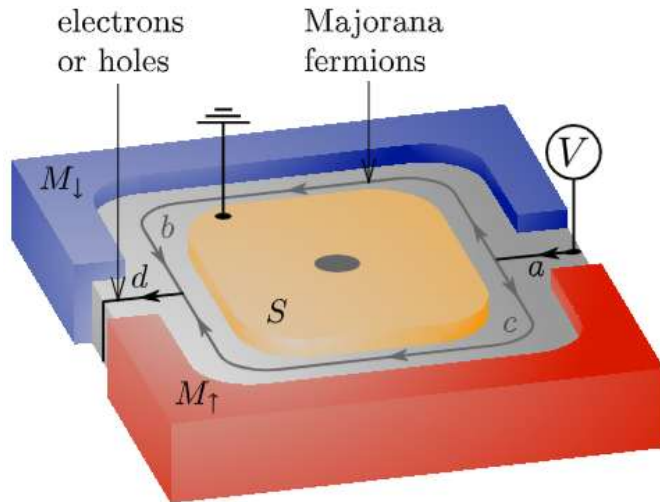
Electrons are incident at  $E = eV$



# MQT in action: $\frac{dI}{dV}$ of topological system from S-matrix

- Physical pictures

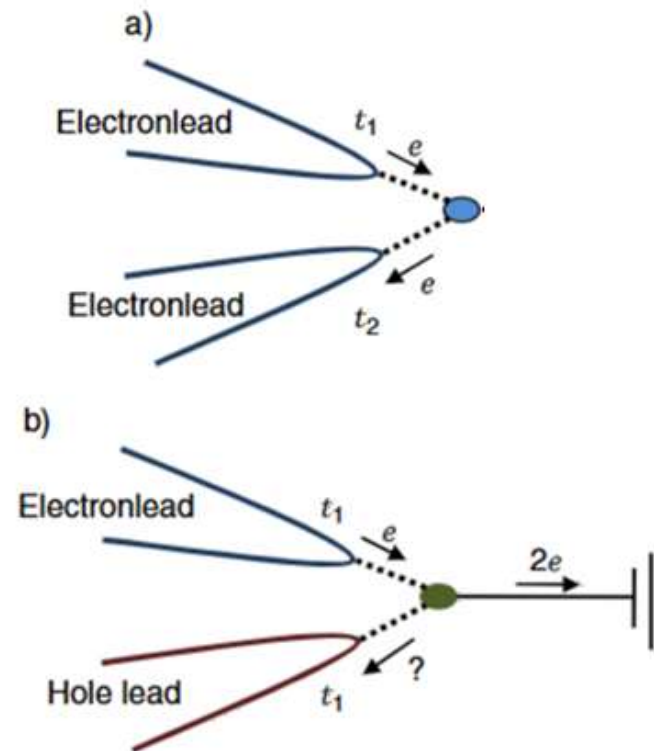
Electrically Detected  
Interferometry of Majorana  
Fermions in a TI  
PRL **102**, 216404 (2009)



$$c_a^{\dagger} \rightarrow \gamma_b + i\gamma_c,$$

$$c_a \rightarrow \gamma_b - i\gamma_c.$$

Majorana Fermion Induced  
Resonant Andreev Reflection  
PRL **103**, 237001 (2009)



# What left beyond today's lecture

- **More about Landauer-Büttiker formalism**

- MQT is quantal: DC current =  $\langle \hat{I} \rangle$ , i.e., long-time average of current
- Current shot noise is also available [M. Büttiker, *PRB* **46**, 12485 (1992)]
- Periodically driven quantum pumps can be dealt [M. Büttiker, (1990)]

- **Beyond Landauer-Büttiker formalism: other methods for MQT**

Formalisms	Advantages	Disadvantages
Landauer-Büttiker	Intuitive & quick calculations. Finite voltage bias & temperature	Cannot deal with many-body physics
Kubo's linear response theory	Relatively easy & quick, while allowing many-body physics	Only allows physics around equilibrium states
Master equation	Allowing many-body physics & Nonequilibrium bias & finite temp.	Particularly useful at tunneling regime
Keldysh formalism	All the above	Not so easy for everyone